

aneurysm of the left middle cerebral artery. The patient's mother suffered from dementia, but the details of her disease were unknown. The patient substituted words for names of people and objects. Two years after the onset of symptoms, the patient became severely disfluent. However, she did not show any violent behavior, personality changes, or other behavioral abnormalities. The patient scored 29/30 on the MMSE. On the frontal assessment battery, she scored 13/18. The patient's time to complete the Trail Making Test (TMT) A was 70 s, and she could not finish the TMT B within five minutes. Her spontaneous speech production was characterized by slow and hesitant speech, frequently interrupted by long word-finding pauses. Her motor speech abilities were within the normal limits, and no apraxia of speech was noted. No parkinsonism was observed. The patient's clinical diagnosis was PPA with a family history of dementia.

### 3.3. Results of *C9orf72* analysis

We identified no patients with expanded hexanucleotide repeats in *C9orf72* in this study. In 75 patients, the average repeat number based on fluorescent fragment-length analysis was  $3.77 \pm 2.56$  (range 2–11 repeats). We have previously reported that an analysis of 197 Japanese healthy controls did not find any *C9orf72* mutation. The average repeat number was  $3.69 \pm 2.46$  (range 2–14 repeats) in the 197 controls [21].

## 4. Discussion

We identified five *MAPT* mutations, including a novel *de novo* mutation and a novel *PGRN* mutation, and we found no *C9orf72* mutations in our 75 patients. More mutations were found in *MAPT* than in the other two genes evaluated in this study. The infrequent observation of *PGRN* and *C9orf72* mutations might be partly due to the small number of FTLD patients included ( $n = 38$ ) because the majority of *PGRN* and *C9orf72* mutations have been described in patients with FTLD. In contrast to most other mutation screening studies, we performed MLPA analysis to ensure that exonic or larger deletions or multiplications of *MAPT* and *PGRN* would be identified. Therefore, our data also show that multiplications of *MAPT* and exonic or genomic deletions in *PGRN* are rare in Asian populations. Although mutations were detected in FTLD and PSP patients, we did not find any mutations in our CBS patients. A further larger study and investigation of the other genes are needed to clarify the genetic background of Japanese patients with CBS.

The *MAPT* p.S285R mutation, which we found in this study, is a novel *de novo* mutation. To the best of our knowledge, this report is the first description of an adult sporadic case of a *de novo* *MAPT* mutation associated with dementia and parkinsonism. All six patients (Patients 1, 2, 3, 5, 6, and 7) with PSP and the distinct eye movements described in the present study (such as tonic upward ocular fixation, oscillopsia with congenital nystagmus, and visual grasping) harbored *MAPT* mutations. Below, we discuss these abnormal eye movements, which are generally not observed in patients with sporadic PSP.

In Patient 1 (*MAPT* p.S285R), we observed tonic upward ocular fixation, which is a loss of downward saccades resembling an acquired ocular motor apraxia [22]. This condition is characterized by a loss of voluntary control of saccades and pursuit, whereas reflex movements—in particular, the vestibulo-ocular reflex—were preserved. Acquired ocular motor apraxia is usually the result of bilateral frontal or frontoparietal infarcts. Therefore, tonic upward ocular fixation due to a *MAPT* mutation might share “supranuclear” cerebral lesions in common with ocular motor apraxia. Brainstem functions, including the vestibulo-ocular reflex and Bell's phenomenon, were preserved in Patient 1.

In Patients 2 and 3 (*MAPT* p.N279K), pendular nystagmus was present since childhood and was suppressed with eyelid closure. These features are consistent with congenital nystagmus [23]. Most patients with congenital nystagmus do not complain of oscillopsia, despite having nearly continuous eye movement [23]. Notably, Patients 2 and 3 noticed oscillopsia when they developed parkinsonism. In these siblings, cerebral lesions caused solely by a *MAPT* mutation were unlikely to be the cause of their nystagmus; however, the co-existence of congenital nystagmus and the *MAPT* mutation might have caused the oscillopsia. This notion is supported in part because the patients had a sister who remained healthy—even in her late 60s—and did not complain of oscillopsia, despite having obvious pendular nystagmus (Fig. 1A). Thus, *MAPT* mutations might impair the visual-motion processing pathways that would normally suppress oscillopsia in patients with common congenital nystagmus. Visual grasping, which was first described by Ghika et al. [20], was observed in Patients 5, 6, and 7 (*MAPT* p.N279K) [19].

Although PSP is a rare manifestation of *MAPT* mutation [24], and the routine screening of sporadic PSP for mutations in *MAPT* is not recommended because of low yield [25], it is recommended that screening be considered for families in which there is an autosomal dominant history of a PSP syndrome, particularly when there are accompanying features suggestive of bvFTD [24]. The clinical difference from sporadic PSP might sometimes be difficult to detect, especially in patients without a family history [26–28]; however, an important case report indicated that an age at disease onset under 50 years combined with the absence of early falling may indicate a possible *MAPT* mutation in clinically diagnosed PSP, even in the absence of a positive family history [26]. Consistent with this observation, our eight *MAPT*-positive patients with PSP phenotype were younger than 50 years at disease onset (Table 2). We further suggest that it may be useful to test for *MAPT* mutations in early-onset PSP patients with the abnormal eye movements that are not typical of sporadic PSP. In fact, we identified the novel *de novo* mutation p.S285R in Patient 1 and p.N279K in Patient 5, who had no family history, after focusing on these clinical phenotypes.

To the best of our knowledge, the *PGRN* mutation has not been previously described in Asian populations [29]. We detected a novel *PGRN* mutation, p.G338RfsX23 (c.1012\_1013delGGinsC), and thus showed that *PGRN* mutations may exist in Asian populations. This mutation introduces a premature termination codon at the same site as the p.G333VfsX28 (c.998delG) mutation, which was reported previously, and produced a PPA phenotype in all of the affected individuals [30]. The PPA phenotype of p.G338RfsX23 (c.1012\_1013delGGinsC) in our study is remarkably similar to that of p.G333VfsX28 (c.998delG), especially in the manifestation of word-finding and object-naming difficulties and the lack of memory or personality changes during the first few years after symptom onset. We believe that the mutant RNA in both cases is most likely subjected to nonsense-mediated decay, similar to other *PGRN* mutations [2].

In summary, based on these findings, we recommend genetic testing for *MAPT* mutations not only in familial patients but also in sporadic patients, especially early-onset PSP patients with the abnormal eye movements that are generally not observed in sporadic PSP. Although *PGRN* and *C9orf72* mutations were rare in this study, we determined that the *PGRN* mutation does exist in Asian patients with FTLD (PPA). Based on the clinical information, screening for *MAPT*, *PGRN*, and *C9orf72* mutations should be further undertaken to improve the diagnosis of specific clinical entities of neurodegenerative disorders.

### Conflicts of interest

None.

## Acknowledgments

The authors thank all of the participants in this study. The authors also thank Dr. Mariely DeJesus-Hernandez for technical advice on the analysis of *C9orf72* repeat expansion. This work was supported by the Strategic Research Foundation Grant-in-Aid Project for Private Universities, Grants-in-Aid for Scientific Research, Grant-in-Aid for Young Scientists, and Grant-in-Aid for Scientific Research on Innovative Areas from the Japanese Ministry of Education, Culture, Sports, Science and Technology, Grants-in-Aid from the Research Committee of CNS Degenerative Diseases and Muro Disease (Kii ALS/PDC), Grants-in-Aid from the Research Committee on CNS Degenerative Diseases and Perry Syndrome from the Ministry of Health, Labor and Welfare of Japan, Project Research Grants-in-Aid from Juntendo University School of Medicine, and CREST from the Japan Science and Technology Agency (JST).

## Appendix A. Supplementary data

Supplementary data related to this article can be found online at <http://dx.doi.org/10.1016/j.parkreldis.2012.06.019>.

## References

- [1] Hutton M, Lendon CL, Rizzu P, Baker M, Froelich S, Houlden H, et al. Association of missense and 5'-splice-site mutations in tau with the inherited dementia FTDP-17. *Nature* 1998;393:702–5.
- [2] Baker M, Mackenzie IR, Pickering-Brown SM, Gass J, Rademakers R, Lindholm C, et al. Mutations in progranulin cause tau-negative frontotemporal dementia linked to chromosome 17. *Nature* 2006;442:916–9.
- [3] Cruts M, Gijssels L, van der Zee J, Engelborghs S, Wils H, Pirici D, et al. Null mutations in progranulin cause ubiquitin-positive frontotemporal dementia linked to chromosome 17q21. *Nature* 2006;442:920–4.
- [4] DeJesus-Hernandez M, Mackenzie IR, Boeve BF, Boxer AL, Baker M, Rutherford NJ, et al. Expanded GGGGCC hexanucleotide repeat in noncoding region of C9ORF72 causes chromosome 9p-linked FTD and ALS. *Neuron* 2011;72:245–56.
- [5] Renton AE, Majounie E, Waite A, Simon-Sanchez J, Rollinson S, Gibbs JR, et al. A hexanucleotide repeat expansion in C9ORF72 is the cause of chromosome 9p21-Linked ALS-FTD. *Neuron* 2011;72:257–68.
- [6] Boeve BF, Hutton M. Refining frontotemporal dementia with parkinsonism linked to chromosome 17: introducing FTDP-17 (MAPT) and FTDP-17 (PGRN). *Arch Neurol* 2008;65:460–4.
- [7] Murray ME, DeJesus-Hernandez M, Rutherford NJ, Baker M, Duara R, Graff-Radford NR, et al. Clinical and neuropathologic heterogeneity of c9FTD/ALS associated with hexanucleotide repeat expansion in C9ORF72. *Acta Neuropathol* 2011;122:673–90.
- [8] Lindquist S, Duno M, Batbayli M, Puschmann A, Braendgaard H, Mardosiene S, et al. Corticobasal and ataxia syndromes widen the spectrum of C9ORF72 hexanucleotide expansion disease. *Clin Genetics* 2012 May 31 [Epub ahead of print].
- [9] Neary D, Snowden JS, Gustafson L, Passant U, Stuss D, Black S, et al. Frontotemporal lobar degeneration: a consensus on clinical diagnostic criteria. *Neurology* 1998;51:1546–54.
- [10] Mesulam MM. Slowly progressive aphasia without generalized dementia. *Ann Neurol* 1982;11:592–8.
- [11] Litvan I, Agid Y, Calne D, Campbell G, Dubois B, Duvoisin RC, et al. Clinical research criteria for the diagnosis of progressive supranuclear palsy (Steele-Richardson-Olszewski syndrome): report of the NINDS-SPSP international workshop. *Neurology* 1996;47:1–9.
- [12] Boeve BF, Lang AE, Litvan I. Corticobasal degeneration and its relationship to progressive supranuclear palsy and frontotemporal dementia. *Ann Neurol* 2003;54(Suppl. 5):S15–9.
- [13] Baker M, Kwok JB, Kucera S, Crook R, Farrer M, Houlden H, et al. Localization of frontotemporal dementia with parkinsonism in an Australian kindred to chromosome 17q21-22. *Ann Neurol* 1997;42:794–8.
- [14] Keyser RJ, Lombard D, Veikondis R, Carr J, Bardin S. Analysis of exon dosage using MLPA in South African Parkinson's disease patients. *Neurogenetics* 2010;11:305–12.
- [15] Varani L, Hasegawa M, Spillantini MG, Smith MJ, Murrell JR, Ghetti B, et al. Structure of tau exon 10 splicing regulatory element RNA and destabilization by mutations of frontotemporal dementia and parkinsonism linked to chromosome 17. *Proc Natl Acad Sci U S A* 1999;96:8229–34.
- [16] Kobayashi T, Ota S, Tanaka K, Ito Y, Hasegawa M, Umeda Y, et al. A novel L266V mutation of the tau gene causes frontotemporal dementia with a unique tau pathology. *Ann Neurol* 2003;53:133–7.
- [17] Clark LN, Poorkaj P, Wszolek Z, Geschwind DH, Nasreddine ZS, Miller B, et al. Pathogenic implications of mutations in the tau gene in pallido-ponto-nigral degeneration and related neurodegenerative disorders linked to chromosome 17. *Proc Natl Acad Sci U S A* 1998;95:13103–7.
- [18] Spillantini MG, Yoshida H, Rizzini C, Lantos PL, Khan N, Rossor MN, et al. A novel tau mutation (N296N) in familial dementia with swollen achromatic neurons and corticobasal inclusion bodies. *Ann Neurol* 2000;48:939–43.
- [19] Ogaki K, Motoi Y, Li Y, Tomiyama H, Shimizu N, Takanashi M, et al. Visual grasping in frontotemporal dementia and parkinsonism linked to chromosome 17 (microtubule-associated with protein tau): a comparison of N-Iso-propyl-p-[(123)I]-iodoamphetamine brain perfusion single photon emission computed tomography analysis with progressive supranuclear palsy. *Mov Disord* 2011;26:561–3.
- [20] Ghika J, Tennis M, Growdon J, Hoffman E, Johnson K. Environment-driven responses in progressive supranuclear palsy. *J Neurol Sci* 1995;130:104–11.
- [21] Ogaki K, Li Y, Atsuta N, Tomiyama H, Funayama M, Watanabe H, et al. Analysis of C9orf72 repeat expansion in 563 Japanese patients with ALS. *Neurobiol Aging* 2012 June 21 [Epub ahead of print].
- [22] Pierrat-Deseilligny C, Gautier JC, Loron P. Acquired ocular motor apraxia due to bilateral frontoparietal infarcts. *Ann Neurol* 1988;23:199–202.
- [23] Leigh RJZD. In: *The neurology of eye movements*. 4 ed. New York: Oxford University Press; 2006. p. 512–21, 638–45.
- [24] Rohrer JD, Paviour D, Vandrovicova J, Hodges J, de Silva R, Rossor MN. Novel L284R MAPT mutation in a family with an autosomal dominant progressive supranuclear palsy syndrome. *Neurodegener Dis* 2011;8:149–52.
- [25] Williams DR, Pittman AM, Revesz T, Lees AJ, de Silva R. Genetic variation at the tau locus and clinical syndromes associated with progressive supranuclear palsy. *Mov Disord* 2007;22:895–7.
- [26] Morris HR, Osaki Y, Holton J, Lees AJ, Wood NW, Revesz T, et al. Tau exon 10 + 16 mutation FTDP-17 presenting clinically as sporadic young onset PSP. *Neurology* 2003;61:102–4.
- [27] Rossi G, Gasparoli E, Pasquali C, Di Fede G, Testa D, Albanese A, et al. Progressive supranuclear palsy and Parkinson's disease in a family with a new mutation in the tau gene. *Ann Neurol* 2004;55:448.
- [28] Ros R, Thobois S, Streichenberger N, Kopp N, Sanchez MP, Perez M, et al. A new mutation of the tau gene, G303V, in early-onset familial progressive supranuclear palsy. *Arch Neurol* 2005;62:1444–50.
- [29] Kim HJ, Jeon BS, Yun JY, Seong MW, Park SS, Lee JY. Screening for MAPT and PGRN mutations in Korean patients with PSP/CBS/FTD. *Parkinsonism Relat Disord* 2010;16:305–6.
- [30] Mesulam MM. Primary progressive aphasia—a language-based dementia. *N Engl J Med* 2003;349:1535–42.
- [31] Imai Y, Hasegawa K. The revised hasegawa's dementia scale (HDS-R) — evaluation of its usefulness as a screening test for dementia. *J Hong Kong Coll Psychiatr* 1994;4:20–4.



## Tricornered/NDR kinase signaling mediates PINK1-directed mitochondrial quality control and tissue maintenance

Zhihao Wu, Tomoyo Sawada, Kahori Shiba, et al.

*Genes Dev.* 2013 27: 157-162

Access the most recent version at doi:10.1101/gad.203406.112

---

**Supplemental Material**

<http://genesdev.cshlp.org/content/suppl/2013/01/24/27.2.157.DC1.html>

**References**

This article cites 37 articles, 12 of which can be accessed free at:  
<http://genesdev.cshlp.org/content/27/2/157.full.html#ref-list-1>

**Email Alerting Service**

Receive free email alerts when new articles cite this article - sign up in the box at the top right corner of the article or [click here](#).

---

---

To subscribe to *Genes & Development* go to:  
<http://genesdev.cshlp.org/subscriptions>

---

## RESEARCH COMMUNICATION

## Tricornered/NDR kinase signaling mediates PINK1-directed mitochondrial quality control and tissue maintenance

Zhihao Wu,<sup>1</sup> Tomoyo Sawada,<sup>2,3</sup> Kahori Shiba,<sup>4</sup> Song Liu,<sup>1</sup> Tomoko Kanao,<sup>5</sup> Ryosuke Takahashi,<sup>2,3</sup> Nobutaka Hattori,<sup>4,5,6</sup> Yuzuru Imai,<sup>6,7</sup> and Bingwei Lu<sup>1,7</sup>

<sup>1</sup>Department of Pathology, Stanford University School of Medicine, Stanford, California 94305, USA; <sup>2</sup>Department of Neurology, Graduate School of Medicine, Kyoto University, Kyoto 606-8507, Japan; <sup>3</sup>CREST (Core Research for Evolutionary Science and Technology), Japan Science and Technology Agency, Saitama 332-0012, Japan; <sup>4</sup>Department of Neurology, Juntendo University Graduate School of Medicine, Tokyo 113-8421, Japan; <sup>5</sup>Research Institute for Diseases of Old Age, Juntendo University Graduate School of Medicine, Tokyo 113-8421, Japan; <sup>6</sup>Department of Neuroscience for Neurodegenerative Disorders, Juntendo University Graduate School of Medicine, Tokyo 113-8421, Japan

**Eukaryotes employ elaborate mitochondrial quality control (MQC) to maintain the function of the power-generating organelle. Parkinson's disease-associated PINK1 and Parkin actively participate in MQC. However, the signaling events involved are largely unknown. Here we show that mechanistic target of rapamycin 2 (mTORC2) and Tricornered (Trc) kinases act downstream from PINK1 to regulate MQC. Trc is phosphorylated in mTORC2-dependent and mTORC2-independent manners and is specifically localized to mitochondria in response to PINK1, which regulates mTORC2 through mitochondrial complex-I activity. Genetically, mTORC2 and Trc act upstream of Parkin. Thus, multiplex kinase signaling is acting between PINK1 and Parkin to regulate MQC, a process highly conserved in mammals.**

Supplemental material is available for this article.

Received August 13, 2012; revised version accepted December 4, 2012.

To sustain energy supply and overall cellular health, elaborate quality control systems are deployed to maintain mitochondrial integrity and functionality (Narendra and Youle 2011; Rugarli and Langer 2012). Mitochondrial quality control (MQC) is particularly important for the maintenance of neural and muscular tissues. PINK1

(Valente et al. 2004) and Parkin (Kitada et al. 1998), two proteins associated with familial Parkinson's disease (PD), have been identified as central players in a cellular pathway that directs MQC, a dynamic and multifaceted network encompassing mitochondrial complex-I (CI) function (Liu et al. 2011; Vilain et al. 2012), fission/fusion dynamics (Yang et al. 2008), transport (Wang et al. 2011; Liu et al. 2012), and mitophagy (Liu and Lu 2010; Narendra et al. 2010). Genetic epistasis studies, first in *Drosophila* (Clark et al. 2006; Park et al. 2006; Yang et al. 2006) and later in mammalian cells (Exner et al. 2007), positioned PINK1 upstream of Parkin in MQC. Studies in mammalian cells have further shown that PINK1 becomes stabilized on the outer membrane of depolarized mitochondria, where it recruits Parkin from the cytosol to promote mitophagy (Narendra et al. 2010). However, the mechanisms of PINK1 and Parkin action and the signaling events involved in the MQC process are poorly understood, with various discordant models having been proposed (Narendra and Youle 2011).

We continued using the powerful tools available in *Drosophila* to dissect the genetic program underlying PINK1/Parkin-directed MQC. Here we identify mechanistic target of rapamycin 2 (mTORC2) and tricornered (Trc) kinase signaling as intermediate steps between PINK1 and Parkin in the MQC process in *Drosophila* and further verify the findings in mammalian cells. Our results reveal a previously unanticipated complexity of signaling events involved in PINK1/Parkin-directed MQC and tissue maintenance and shed new light on how mTORC2 and Trc, two important kinases critically involved in cellular morphogenesis, development, growth, and disease, are regulated in an in vivo setting.

### Results and Discussion

To elucidate the signaling events acting downstream from PINK1, we performed genetic screens as described before (Liu and Lu 2010; Liu et al. 2012) to identify genes that can modify PINK1 loss-of-function (LOF)-induced wing posture and flight ability defects. This led to the identification of mTORC2 components as strong modifiers of PINK1. While overexpression of the mTORC2 components Rictor and Sin1 (Hietakangas and Cohen 2007), either individually or in combination, had no obvious effects on their own (Supplemental Fig. S1), they effectively suppressed *dpink1* LOF phenotypes with respect to the integrity and function of flight muscle, as measured by thoracic ATP level and wing posture (Fig. 1A,B; Supplemental Fig. S1D) and the loss of dopaminergic neurons (DNs) in the PPL1 cluster (Fig. 1E). Conversely, *rictor* or *sin1* mutations significantly enhanced *dpink1* LOF phenotypes (Fig. 1A–E; Supplemental Fig. S1D), although the *rictor* or *sin1* mutant alone did not show obvious phenotypes in these assays (Supplemental Fig. S1A–C). The effects of mTORC2 components on tissue integrity correlated well with the effects on mitochondrial morphology, with mTORC2 gain of function (GOF) rescuing the mitochondrial aggregation phenotype caused by *dpink1* LOF, whereas mTORC2 LOF had opposite effects (Fig. 1C,D).

We next explored the molecular mechanisms underlying the strong genetic interaction between PINK1 and mTORC2. Using phosphorylation of *Drosophila* AKT at S505 as readout of mTORC2 activity (Sarbasov et al.

[**Keywords:** Tricornered, NDR, mTORC2, PINK1, mitochondrial quality control]

<sup>7</sup>Corresponding authors

E-mail bingwei@stanford.edu

E-mail yzimai@juntendo.ac.jp

Article is online at <http://www.genesdev.org/cgi/doi/10.1101/gad.203406.112>.

Wu et al.

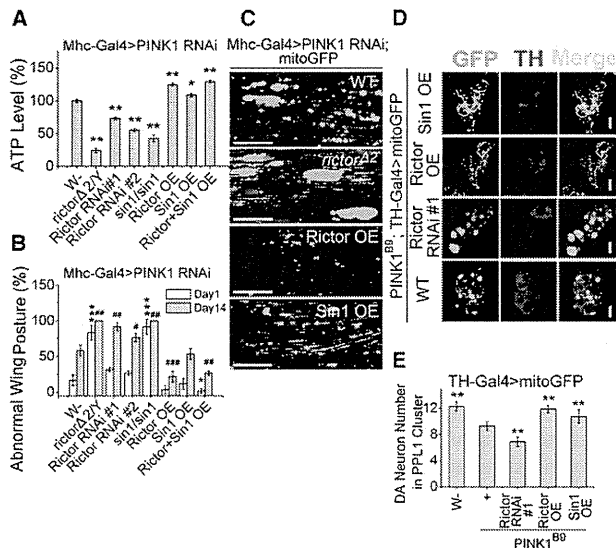


**Figure 1.** Genetic interaction between PINK1 and mTORC2. (A) PINK1 RNAi-induced ATP level drop was rescued by *Rictor* or *Sin1* overexpression (OE) but enhanced by their LOF. (B) PINK1 RNAi-induced abnormal wing posture was rescued by *Rictor* overexpression or *Rictor* + *Sin1* overexpression but enhanced by their LOF. (C) PINK1 RNAi-induced mitochondrial aggregation in muscle was strongly rescued by *Rictor* overexpression and moderately rescued by *Sin1* overexpression but was enhanced by *rictor* LOF. Mitochondrial morphology was monitored with a mito-GFP reporter. Bar, 30  $\mu$ m. (D) PINK1 LOF-induced mitochondrial aggregation in DNs was strongly rescued by *Rictor* overexpression and moderately rescued by *Sin1* overexpression but enhanced by *rictor* LOF. Bar, 5  $\mu$ m. (E) PINK1 LOF-induced loss of DNs in the PPL1 cluster was rescued by *Rictor* overexpression but enhanced by *rictor* LOF. A *rictor* deletion mutant ( $\Delta$ 2) and two independent *rictor* RNAi lines (#1 and #2) were used in LOF studies. (\* or #)  $P < 0.05$ ; (\*\* or ##)  $P < 0.01$ ; (\*\*\*) or ###)  $P < 0.005$  in one-way ANOVA tests when data from day 1 or day 14 were compared.

2005), we found that the p-S505-AKT level was significantly reduced in the *dpink1* LOF condition but increased by PINK1 GOF (Fig. 2A), indicating that PINK1 regulates mTORC2 activity in vivo. To further validate this point, we affinity-purified *Drosophila* mTORC2 from transgenic animals expressing a Flag-tagged *Sin1* (Koike-Kumagai et al. 2009). In vitro kinase assays using purified mTORC2 as the kinase and kinase-dead (KD) GST-AKT as the substrate showed that the specific activity of mTORC2 was reduced in the *dpink1*<sup>B9</sup>-null mutant but increased in PINK1 GOF background (Fig. 2B). The amounts of dTOR copurifying with Flag-*Sin1* were comparable among the various genotypes (Fig. 2B), suggesting that PINK1 primarily regulates mTORC2 kinase activity instead of its assembly. Consistent with impaired mTORC2 signaling contributing to PINK1 pathogenesis, phosphatidylinositol 3,4,5-trisphosphate (PIP<sub>3</sub>) treatment, which could directly activate mTORC2 in mammalian cells (Gan et al. 2011), partially restored mTORC2 activity (Fig. 2C,D) and rescued *dpink1* mutant phenotypes in terms of lifespan, wing posture, and mitochondrial morphology (Fig. 2E–G).

Despite the importance of mTORC2 in physiology and disease, little is known about how it is regulated by upstream signals (Zoncu et al. 2011). We further investigated how PINK1 regulates mTORC2 activity. Given that PINK1 is a mitochondrial resident protein intimately linked to CI function and that CI dysfunction could phenocopy *dpink1* LOF effects (Supplemental Fig. S2A–C), we

reasoned that the functional status of CI might affect mTORC2 activity. To test this hypothesis, we first examined p-S505-AKT levels in wild-type animals treated with the CI inhibitor rotenone (Fig. 2H) or with CI subunits knocked down by RNAi (Fig. 2I). These manipulations led to decreased p-S505-AKT levels. Consistently, mTORC2 purified from CI-impaired animals exhibited reduced kinase activity in vitro (Supplemental Fig. S2D). Importantly, in *dpink1* mutants whose CI activity was supplemented by yeast NADH ubiquinone oxidoreductase (*yNDI1*), the mutant phenotypes were effectively rescued (Supplemental Fig. S2E–G), consistent with a recent study (Vilain et al. 2012), and p-S505-AKT level was restored to normal (Fig. 2I). Further supporting a functional link between CI and mTORC2 activation, mTORC2 LOF animals were particularly sensitive to rotenone treatment compared with other stress treatments (Supplemental Fig. S3A–F), and LOF of mTORC2 and CI synergistically disrupted muscle function (Supplemental Fig. S3G). These results demonstrate that the functional state of CI maintained by PINK1 is a critical determinant of mTORC2 activity. Supporting this notion, PINK1 was found to associate with components of CI (Supplemental Fig. S2H).

Next, we sought to determine the signaling events downstream from mTORC2 that mediate PINK1-directed MQC and tissue maintenance. Surprisingly, even though AKT is considered a key downstream target of mTORC2 (Wullschlegel et al. 2006; Russell et al. 2011; Zoncu et al. 2011) and AKT function is compromised in the *dpink1* mutant, as shown by a reduced p-S505-AKT level, overexpression of wild-type or phospho-mutant forms of AKT had no obvious effect on *dpink1* LOF phenotypes in terms of mitochondrial morphology and tissue maintenance (Supplemental Fig. S4A–C). Knocking down AKT by RNAi also had no obvious effect (Supplemental Fig. S4A–C). Thus, the best-studied mTORC2 target, AKT, is unlikely to be a key mediator of mTORC2 function in PINK1-controlled MQC and tissue maintenance.

Trc kinase was recently identified as a downstream effector of mTORC2 in regulating the dendritic tiling of *Drosophila* sensory neurons (Koike-Kumagai et al. 2009). Trc was originally isolated in a screen for genes affecting wing hair morphogenesis (Geng et al. 2000) and was later found to be important for dendritic patterning (Emoto et al. 2004) in *Drosophila*. Trc is homologous to mammalian nuclear Dbf-2-related (NDR) kinases (Hergovich et al. 2006). Whether Trc/NDR regulates mitochondrial function or neuromuscular tissue maintenance is not known. Interestingly, although overexpression of Trc LOF or GOF transgenes alone had little effect on muscle function (Supplemental Fig. S5A–C), Trc GOF transgenes effectively suppressed *dpink1* LOF phenotypes in muscle (Fig. 3A,B; Supplemental Fig. S5D) or DN (Fig. 3E) maintenance and mitochondrial morphology (Fig. 3C,D), whereas dominant-negative Trc (Trc-K122A or Trc-K122/T453A) had opposite effects (Fig. 3A–E; Supplemental Fig. S5D). Note that wild-type or constitutively active Trc (Trc-S292E and Trc-T453E) were equally effective in the GOF assays, indicating that overexpressed wild-type Trc became sufficiently activated, as indicated by its high level phosphorylation at S292 (Fig. 3F).

Consistent with Trc acting downstream from mTORC2, the enhancement of *dpink1* LOF phenotypes by *rictor* mutation was attenuated by wild-type Trc (Trc-WT) or Trc-S292E GOF transgenes (Supplemental Fig. S6A,C),

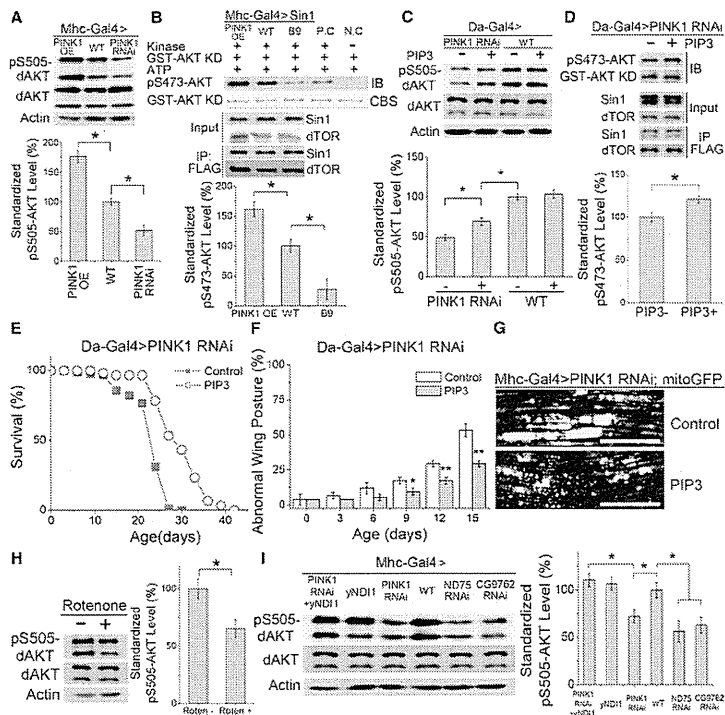


**Figure 2.** Effects of PINK1 and mitochondrial CI function on TORC2 activity. (A) Western blot analysis of *Mhc-Gal4*-driven control (wild type [WT]), PINK1 overexpression, and PINK1-RNAi muscle extracts with the indicated antibodies and data quantification. (B, top) In vitro phosphorylation of recombinant human GST-AKT-KD by *Drosophila* TORC2 affinity-purified from control, PINK1-overexpressing, and PINK1 LOF animals, all expressing a Sin1-Flag transgene. (Bottom) Similar amounts of Sin1 and dTOR were present in the extracts or immunoprecipitated TORC2. After kinase reaction, AKT phosphorylation was detected with anti-pS473-AKT, and total GST-AKT-KD was detected by Coomassie Blue staining (CBS). (P.C.) Positive control with extract added; (N.C.) negative control with no kinase added. Bar graph shows data quantification. (C–G) The rescuing effect of PIP3 treatment on in vivo p-S505-AKT level (C), in vitro mTORC2 kinase activity (D), lifespan (E), wing posture (F), and muscle mitochondrial morphology (G) in PINK1-RNAi animals. Values represent relative protein amounts after normalization with controls. Mitochondrial morphology was monitored with a mito-GFP reporter. In vitro mTORC2 kinase assay was performed as in B. Bar graphs show data quantification. Bar, 30  $\mu$ m. (H) Reduction of pS505-AKT level by rotenone treatment of wild-type animals. (I) Effect of CI subunit (ND75 and CG9762) RNAi on pS505-AKT level and restoration of the p-S505-AKT level in PINK1-RNAi animals after yND11 coexpression. Values represent relative protein amounts after normalization with controls. Bar graphs show data quantification. (\*)  $P < 0.05$  in one-way ANOVA or Student's *t*-tests.

whereas the rescue of *dPINK1* LOF phenotypes by Rictor overexpression was fully blocked by Trc LOF transgenes (Supplemental Fig. S6B,D). Moreover, Trc RNAi induced mitochondrial aggregation and DN loss in a wild-type background (Supplemental Fig. S7A–C). These results thus establish Trc as a key component of the PINK1 pathway in MQC and tissue maintenance.

We further explored the biochemical mechanism of the signaling events involving PINK1, mTORC2, and Trc. Consistent with Trc acting downstream from PINK1, phosphorylation of Trc at S292 and T453, which correlate with Trc activation (Emoto et al. 2006), were reduced in *dPINK1* mutants but significantly increased in PINK1 GOF flies (Fig. 3F). This was further supported by in vitro assays of kinase activities of Trc purified from PINK1 LOF and GOF flies using phosphorylation of AAK1, a newly

identified substrate of mammalian NDR (Ultanir et al. 2012), as readout (Fig. 3G). Interestingly, the effect of PINK1 on T453 site phosphorylation was mTORC2-dependent, whereas its effect on S292 was mTORC2-independent (Fig. 3H), suggesting that PINK1 regulates these two phosphorylation events through distinct mechanisms. We next tested whether activated Trc is localized to mitochondria to exert its effects on MQC. Strikingly, p-T453-Trc and p-S292-Trc were found primarily in the mitochondrial fraction, whereas total Trc was found in both the cytoplasmic and mitochondrial fractions (Supplemental Fig. S8A). Since mTORC2 is also localized to mitochondria (Supplemental Fig. S8B), mitochondria may serve as a novel platform for mTORC2 and Trc signaling.

Parkin plays a critical role in MQC and maintenance of muscle and DN and acts downstream from PINK1. We found that the LOF effects of Rictor (Fig. 4A,E) or Trc (Fig. 4C,G) in enhancing *dPINK1* mutant phenotypes were completely blocked by Parkin GOF, suggesting that Parkin acts downstream from TORC2 and Trc in the PINK1 pathway. Consistently, Rictor GOF (Fig. 4B,F) or Trc GOF (Fig. 4D,H) failed to rescue the abnormal wing posture and mitochondrial morphology phenotypes of the *parkin* mutant. Next, we tested the genetic interaction between mTORC2/Trc and key executors of MQC known to genetically interact with PINK1, including the mitochondrial fusion protein Marf (Liu and Lu 2010; Ziviani et al. 2010), the autophagy regulator Atg1 (Liu and Lu 2010), and the mitochondrial transport protein Miro (Wang et al. 2011; Liu et al. 2012). Marf RNAi or Atg1 GOF effectively blocked the enhancing effects of mTORC2 LOF (Fig. 4I,J) or Trc LOF (Fig. 4K,L) in the *dPINK1* mutant background. Miro RNAi was also effective, although to a lesser degree (Fig. 4I–L). Together, these genetic epistasis data support critical roles of mTORC2 and Trc in mediating the effect of PINK1 in MQC and tissue maintenance.

In mammalian cells, the PINK1–Parkin pathway also plays central roles in MQC, with Parkin recruited to damaged mitochondria in a PINK1-dependent manner to promote mitophagy (Narendra et al. 2010). We tested whether the mammalian Trc homologs NDR1/2 act in PINK1/Parkin-directed MQC. Knockdown of NDR1 but not NDR2

in HeLa cells led to altered mitochondrial distribution, compromised recruitment of Parkin by PINK1, and delayed clearance of damaged mitochondria (Supplemental Fig. S9A–C). The mitophagy defects induced by NDR1 RNAi were rescued by a siRNA-resistant NDR1 construct (Supplemental Fig. S9B,D). Importantly, we detected reduced phosphorylation of NDR1 at the corresponding T444 site in *PINK1*<sup>−/−</sup> mouse embryonic fibroblasts (MEFs) expressing a kinase-dead form of PINK1 but not wild-type PINK1 (Supplemental Fig. S10). Due to the hypersensitivity of p-NDR1 to endogenous phosphatase activities as previously reported (Koike-Kumagai et al. 2009), treatment with okadaic acid (OA) was needed to reveal the effect of PINK1 on the p-NDR1 level. These results support that NDR1 acts in the PINK1/Parkin pathway in mammals. In carbonyl cyanide m-chlorophe-

Wu et al.

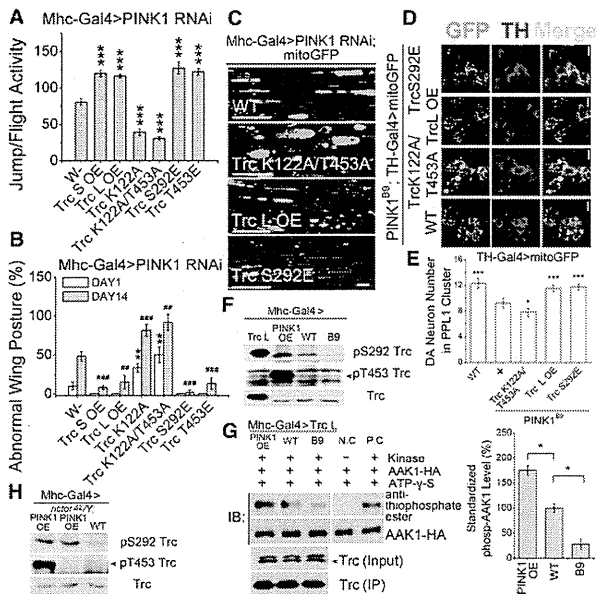


**Figure 3.** Evidence that Trc acts in the PINK1 pathway. (A,B) *Mhc-Gal4>PINK1 RNAi*-induced flight ability (A) and wing posture (B) defects were rescued by the coexpression of the short (S) or long (L) isoforms of wild-type Trc or constitutively active (S292E or T453E) Trc but enhanced by dominant-negative (K122A or K122A/T453A) Trc. (\* or #)  $P < 0.05$ ; (\*\* or ##)  $P < 0.01$ ; (\*\*\*)  $P < 0.005$  in one-way ANOVA tests when data from day 1 (\*) or day 14 (#) were compared. (C) *Mhc-Gal4>PINK1 RNAi*-induced mitochondrial aggregation in indirect flight muscle was rescued by the coexpression of Trc-L or Trc-S292E but enhanced by Trc-K122A/T453A. Mitochondrial morphology was monitored with a mito-GFP reporter. Bar, 30  $\mu\text{m}$ . (D,E) *PINK1*<sup>B9</sup> mutation-induced mitochondrial aggregation in DNns (D) or loss of DNns in the PPL1 clusters (E) was strongly rescued by *TH-Gal4*-driven expression of wild-type or constitutively active Trc but enhanced by dominant-negative Trc. Bar, 5  $\mu\text{m}$ . (F) Western blot analysis showing the effects of *PINK1* LOF or overexpression on Trc phosphorylation. Trc-L overexpression served as a positive control. (G) In vitro kinase assay showing the effects of *PINK1* LOF or overexpression on Trc kinase activity. Trc-L purified from control, *PINK1* mutant, and *PINK1*-overexpressing animals was tested for kinase activity using AAK1-HA as a substrate in the presence of ATP- $\gamma$ -S and phosphorylation detected by anti-thiophosphate ester antibody after esterification with p-nitrobenzylmesylate (PNBM). (P.C.) Positive control with extract added; (N.C.) negative control with no kinase added. Bar graph shows data quantification. (H) Western blot analysis showing that *PINK1*-induced Trc phosphorylation of T453 was Rictor-dependent, whereas that of S292 was Rictor-independent. (\*)  $P < 0.05$ ; (\*\*\*)  $P < 0.005$  in one-way ANOVA tests in E and G.

nylhydrazine (CCCP)-treated HeLa cells, NDR1 was found to colocalize with Parkin and the mitochondrial outer membrane marker Tom 20 (Supplemental Fig. S9B), suggesting that NDR1 might also be localized to mitochondria to exert MQC. In Parkin stably transfected HeLa cells that were subjected to Rictor RNAi (Supplemental Fig. S11A,D) or in *rictor*<sup>-/-</sup> MEF cells (Supplemental Fig. S11B,C,E), the recruitment of Parkin to damaged mitochondria and the kinetics of mitophagy were also delayed, supporting a critical role of mTORC2 in PINK1/Parkin-directed mitophagy in mammals.

We further investigated the mechanism of action of NDR1 in mammalian cells. It has been reported that Parkin is phosphorylated and activated by phosphoryla-

tion upon CCCP treatment (Kondapalli et al. 2012; Shiba-Fukushima et al. 2012). In HeLa cells stably transfected with Parkin, CCCP treatment led to increased phosphorylation of NDR1 and Parkin as detected with Phos tag. NDR1 RNAi significantly attenuated Parkin phosphorylation (Supplemental Fig. S12A), consistent with Parkin acting downstream from NDR1. Further supporting this notion, the activity of Parkin as measured by its auto-ubiquitination was reduced by NDR1 RNAi (Supplemental Fig. S12B). Moreover, the destabilization of MQC-related proteins Mfn1 and Miro1 by CCCP-activated PINK1/Parkin signaling was significantly attenuated by NDR1 RNAi (Supplemental Fig. S12A). These results support the notion that, as in flies, NDR1 kinase signaling acts upstream of Parkin and the other key MQC players in the mammalian MQC pathway.

Our results demonstrate that mTORC2 and Trc signaling are actively involved in the dynamic MQC network directed by PINK1 and that they act between PINK1 and Parkin in a conserved signaling pathway. This finding reveals a previously unappreciated complexity in the signaling steps between PINK1 and Parkin. This is the first time both mTORC2 and Trc are directly implicated in MQC. The fact that PINK1 regulates Trc T453 phosphorylation in an mTORC2-dependent manner and S292 phosphorylation in an mTORC2-independent manner suggests the involvement of additional kinases in this MQC pathway. Our finding of active p-Trc localizing primarily to mitochondria suggests that mitochondria may serve as a key platform for Trc signaling. The kinase that directly acts on Trc T453 in the context studied here remains to be identified. Although mTORC2 is required, it may not be the kinase that directly phosphorylates this site (Koike-Kumagai et al. 2009). Similarly, although PINK1 is required for mTORC2 activation, our results suggest that PINK1 acts through maintaining mitochondrial CI activity to influence mTORC2 activity, rather than directly phosphorylating mTORC2 as proposed in a previous study (Murata et al. 2011). Our findings offer new insights into the novel role of mitochondria in regulating mTORC2 and Trc/NDR kinase signaling.

mTORC2 and Trc signaling both induce cell morphology changes through actin cytoskeleton regulation (Jacinto et al. 2004; Fang and Adler 2010). Given the dynamic changes in mitochondrial distribution and morphology during MQC and the implicated roles of the actin cytoskeleton in regulating mitochondrial distribution and morphology (Boldogh and Pon 2006), it is possible that mTORC2/Trc may act in MQC through cytoskeletal regulation, although this remains to be tested. Our results support the notion that Trc signaling directly impinges on Parkin or the other key MQC executors (Supplemental Fig. S12C). A corollary of our finding is that mitochondrial localization of the kinases and the ensuing MQC may participate in other physiological processes regulated by mTORC2/Trc signaling. Given that deregulated mTORC2 (Zoncu et al. 2011), Trc/NDR (Cornils et al. 2011), and PINK1 and Parkin (Devine et al. 2011) signaling have all been linked to cancer in humans, another important implication of this study is that aberrant MQC signaling also contributes to cancerous growth and that therapeutic agents targeting the newly identified, highly conserved MQC signaling pathway may have broad therapeutic applications.

## Multiplex kinase signaling in the PINK1 pathway

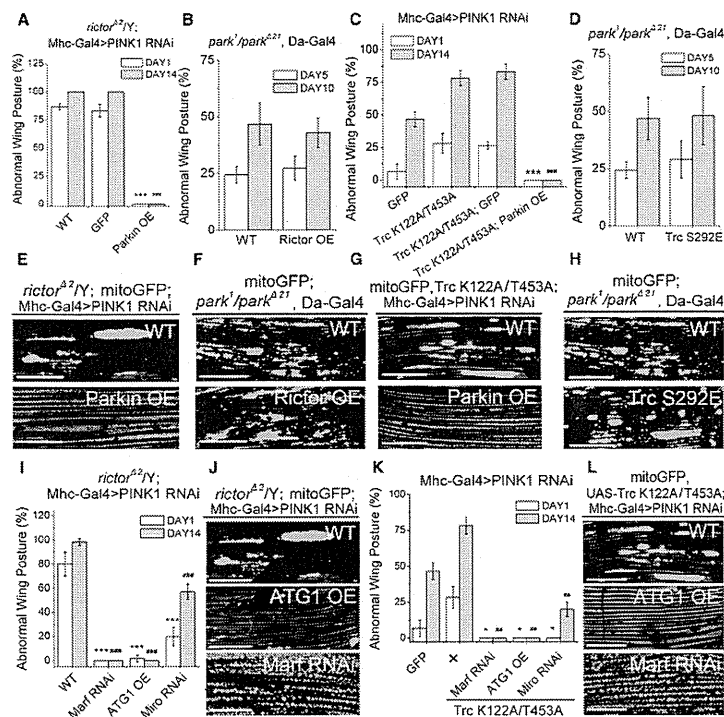


**Figure 4.** Genetic evidence that Parkin and MQC executors act downstream from TORC2 in the PINK1 pathway. (A,E) The enhancement of PINK1 RNAi-induced abnormal wing posture (A) or mitochondrial aggregation (E) by *ricktor* deletion was suppressed by Parkin but not GFP overexpression. (B,F) The rescue of PINK1 RNAi-induced abnormal wing posture (B) or mitochondrial aggregation (F) by Rictor overexpression was blocked by Parkin LOF. (C,G) The enhancement of PINK1 RNAi-induced abnormal wing posture (C) or mitochondrial aggregation (G) by dominant-negative Trc was completely suppressed by Parkin but not GFP overexpression. (D,H) The rescue of PINK1 RNAi-induced abnormal wing posture (D) or mitochondrial aggregation (H) by wild-type or constitutively active Trc was blocked by Parkin LOF. (I,J) The enhancement of PINK1 RNAi-induced abnormal wing posture (I) or mitochondrial aggregation (J) by *ricktor* deletion was suppressed by Miro-RNAi, Marf-RNAi, or Atg1 overexpression. (K,L) The enhancement of PINK1 RNAi-induced abnormal wing posture by dominant-negative Trc was suppressed by Miro-RNAi, Marf-RNAi, or Atg1 overexpression. (\* or #)  $P < 0.05$ ; (\*\* or ##)  $P < 0.01$ ; and (\*\*\*) or ###)  $P < 0.005$  in one-way ANOVA or Student's *t*-tests when data from day 1 (\*) or day 14 (#) were compared. Bars: E–F, J, L, 30  $\mu$ m.

## Materials and methods

## GST fusion protein preparation

The construct expressing human GST-AKT-KD used as the substrate in the in vitro TORC2 kinase assays was a gift from Dr. Dianqing Wu. To avoid autophosphorylation of AKT, the Lys179 and Thr308 residues were mutated (Gan et al. 2011). GST fusion protein was expressed in the *Escherichia coli* BL21 (DE3) strain and purified using glutathione-agarose beads following standard protocols.

## Immunoprecipitation and kinase assay of TORC2

For TORC2 immunoprecipitation, methods adopted from previous studies (Koike-Kumagai et al. 2009; Gan et al. 2011) were used. Briefly, flies were crossed and raised in standard medium at 25°C. Male flies expressing Flag-tagged Sin1 were collected and homogenized in lysis buffer (40 mM HEPES at pH 7.5, 120 mM NaCl, 0.3% CHAPS, 1 mM EDTA, 10 mM  $\beta$ -glycerophosphate, 50 mM NaF, 1 mM PMSF). TORC2 was immunoprecipitated by incubating the supernatant with pre-equilibrated anti-Flag M2 beads (Sigma Aldrich) for 3 h at 4°C. Immunocomplexes were washed

3 times in lysis buffer and twice with the TORC2 kinase buffer (25 mM HEPES at pH 7.5, 100 mM KAc, 2 mM  $MgCl_2$ ). The integrity of the TORC2 was confirmed by Western blot analysis.

For kinase assays, TORC2 immunocomplexes were incubated with 500 ng of human GST-AKT-KD fusion protein in 30  $\mu$ L of TORC2 kinase buffer containing 500  $\mu$ M ATP. The reaction was performed for 30 min at 30°C and terminated by the addition of 30  $\mu$ L of 2 $\times$  SDS sample buffer. AKT phosphorylation by TORC2 was analyzed by Western blot using the p-T473-AKT antibody (Cell Signaling Technology).

## Mitochondrial and cytoplasmic protein fractionation

For mitochondria purification, we adopted a previous method (Kristian et al. 2006). Briefly, fly tissues were collected and homogenized in homogenization buffer (210 mM mannitol, 70 mM sucrose, 1 mM EGTA, 10 mM  $\beta$ -glycerophosphate, 50 mM NaF, 1 mM PMSF, 5 mM HEPES at pH 7.12). The homogenate was centrifuged at 1500g for 5 min, and the supernatant was collected and centrifuged again at 13,000g for 17 min. The supernatant was concentrated as a cytoplasmic protein sample, and the pellet was stored for further mitochondrial purification. For mitochondrial purification, the previous pellet was resuspended in 15% Percoll solution and loaded onto a 15%–22%–50% discontinuous Percoll gradient. The gradient was centrifuged at 30,700g for 6 min, and intact mitochondria were recovered from the 22%–50% gradient interface. Mitochondria were washed with homogenization buffer and subjected to SDS-PAGE.

## Quantitative Western blot analysis

To obtain quantitative Western blot results, experimental conditions such as the amounts of protein loaded, the antibody dilutions, and exposure times were adjusted to make sure that the Western blot signals were in the linear range. For the in vitro kinase assays, Western blot analyses were performed using standard protocols. After incubation with the ECL reagent (PerkinElmer, Inc.), the signals were scanned using a Typhoon 9400 system (GE Healthcare Life Sciences), and signal intensity was quantified by ImageQuantTL. For the other immunoblots, the signals were recorded on X-ray film and scanned, and the signal intensity was analyzed by ImageQuantTL or ImageJ. Statistical analyses were based on data from three independent repeats.

## Statistical analysis

Two-tailed Student's *t*-tests were used in the statistical analysis when comparing two samples. A one-way ANOVA test was used when multiple samples were compared.

## Acknowledgments

We thank Dr. P. Aspenström, Dr. E. Baehrecke, Dr. R. Balogh, Dr. S. Birman, Dr. J. Chung, Dr. S. Cohen, Dr. K. Emoto, Dr. M. Guo, Dr. Y. Hata, Dr. S. Hatakeyama, Dr. B. Hemmings, Dr. Y.N. Jan, Dr. S. Konur, Dr. M. Magnuson, Dr. N. Matsuda, Dr. K. Nakagawa, Dr. W. Saxton, Dr. K. Tanaka, Dr. G. Thomas, Dr. P. Verstreken, Dr. D. Wu, Dr. K. Zinsmaier, Bloomington *Drosophila* Stock Center, Vienna *Drosophila* RNAi Center, and TRiP at Harvard Medical School (NIH/NIGMS R01-GM084947) for flies and reagents, and Lu laboratory members for technical help and discussions. This work was supported by the NIH (R01AR054926 and R01MH080378 to B.L.), Grant-in-Aid for Young Scientists (B) from MEXT in Japan (to Y.I.), the CREST program of JST (to R.T.), a Grant-in-Aid for Scientific Research on Innovative Areas (to R.T.), and a Grant-in-Aid for Science Research from the Ministry of Health, Labor, and Welfare in Japan (to R.T.).

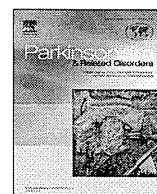
## References

Baldogh IR, Pon LA. 2006. Interactions of mitochondria with the actin cytoskeleton. *Biochim Biophys Acta* 1763: 450–462.



Wu et al.

- Clark IE, Dodson MW, Jiang C, Cao JH, Huh JR, Seol JH, Yoo SJ, Hay BA, Guo M. 2006. *Drosophila* pink1 is required for mitochondrial function and interacts genetically with parkin. *Nature* **441**: 1162–1166.
- Cornils H, Kohler RS, Hergovich A, Hemmings BA. 2011. Downstream of human NDR kinases: Impacting on c-myc and p21 protein stability to control cell cycle progression. *Cell Cycle* **10**: 1897–1904.
- Devine MJ, Plun-Favreau H, Wood NW. 2011. Parkinson's disease and cancer: Two wars, one front. *Nat Rev Cancer* **11**: 812–823.
- Emoto K, He Y, Ye B, Gruber WB, Adler PN, Jan LY, Jan YN. 2004. Control of dendritic branching and tiling by the Tricornered-kinase/Furry signaling pathway in *Drosophila* sensory neurons. *Cell* **119**: 245–256.
- Emoto K, Parrish JZ, Jan LY, Jan YN. 2006. The tumour suppressor Hippo acts with the NDR kinases in dendritic tiling and maintenance. *Nature* **443**: 210–213.
- Exner N, Treske B, Paquet D, Holmström K, Schiesling C, Gispert S, Carballo-Carbajal I, Berg D, Hoepken HH, Gasser T, et al. 2007. Loss-of-function of human PINK1 results in mitochondrial pathology and can be rescued by parkin. *J Neurosci* **27**: 12413–12418.
- Fang X, Adler PN. 2010. Regulation of cell shape, wing hair initiation and the actin cytoskeleton by Trc/Fry and Wts/Mats complexes. *Dev Biol* **341**: 360–374.
- Gan X, Wang J, Su B, Wu D. 2011. Evidence for direct activation of mTORC2 kinase activity by phosphatidylinositol 3,4,5-trisphosphate. *J Biol Chem* **286**: 10998–11002.
- Geng W, He B, Wang M, Adler PN. 2000. The tricornered gene, which is required for the integrity of epidermal cell extensions, encodes the *Drosophila* nuclear DBP2-related kinase. *Genetics* **156**: 1817–1828.
- Hergovich A, Stegert MR, Schmitz D, Hemmings BA. 2006. NDR kinases regulate essential cell processes from yeast to humans. *Nat Rev Mol Cell Biol* **7**: 253–264.
- Hietakangas V, Cohen SM. 2007. Re-evaluating AKT regulation: Role of TOR complex 2 in tissue growth. *Genes Dev* **21**: 632–637.
- Jacinto E, Loewith R, Schmidt A, Lin S, Ruegg MA, Hall A, Hall MN. 2004. Mammalian TOR complex 2 controls the actin cytoskeleton and is rapamycin insensitive. *Nat Cell Biol* **6**: 1122–1128.
- Kitada T, Asakawa S, Hattori N, Matsumine H, Yamamura Y, Minoshima S, Yokochi M, Mizuno Y, Shimizu N. 1998. Mutations in the parkin gene cause autosomal recessive juvenile parkinsonism. *Nature* **392**: 605–608.
- Koike-Kumagai M, Yasunaga K, Morikawa R, Kanamori T, Emoto K. 2009. The target of rapamycin complex 2 controls dendritic tiling of *Drosophila* sensory neurons through the Tricornered kinase signaling pathway. *EMBO J* **28**: 3879–3892.
- Kondapalli C, Kazlauskaitė A, Zhang N, Woodroof HI, Campbell DG, Gourlay R, Burchell L, Walden H, Macartney TJ, Deak M, et al. 2012. PINK1 is activated by mitochondrial membrane potential depolarization and stimulates Parkin E3 ligase activity by phosphorylating Serine 65. *Open Biol* **2**: 120080.
- Kristian T, Hopkins IB, McKenna MC, Fiskum G. 2006. Isolation of mitochondria with high respiratory control from primary cultures of neurons and astrocytes using nitrogen cavitation. *J Neurosci Methods* **152**: 136–143.
- Liu S, Lu B. 2010. Reduction of protein translation and activation of autophagy protect against PINK1 pathogenesis in *Drosophila melanogaster*. *PLoS Genet* **6**: e1001237.
- Liu W, Acín-Peréz R, Geghman KD, Manfredi G, Lu B, Li C. 2011. Pink1 regulates the oxidative phosphorylation machinery via mitochondrial fission. *Proc Natl Acad Sci* **108**: 12920–12924.
- Liu S, Sawada T, Lee S, Yu W, Silverio G, Alapat P, Millan I, Shen A, Saxton W, Kanao T, et al. 2012. Parkinson's disease-associated kinase PINK1 regulates miro protein level and axonal transport of mitochondria. *PLoS Genet* **8**: e1002537.
- Murata H, Sakaguchi M, Jin Y, Sakaguchi Y, Futami J, Yamada H, Kataoka K, Huh NH. 2011. A new cytosolic pathway from a Parkinson disease-associated kinase, BRPK/PINK1: Activation of AKT via mTORC2. *J Biol Chem* **286**: 7182–7189.
- Narendra DP, Youle RJ. 2011. Targeting mitochondrial dysfunction: Role for PINK1 and Parkin in mitochondrial quality control. *Antioxid Redox Signal* **14**: 1929–1938.
- Narendra DP, Jin SM, Tanaka A, Suen DE, Gautier CA, Shen J, Cookson MR, Youle RJ. 2010. PINK1 is selectively stabilized on impaired mitochondria to activate Parkin. *PLoS Biol* **8**: e1000298.
- Park J, Lee SB, Lee S, Kim Y, Song S, Kim S, Bae E, Kim J, Shong M, Kim JM, et al. 2006. Mitochondrial dysfunction in *Drosophila* PINK1 mutants is complemented by parkin. *Nature* **441**: 1157–1161.
- Rugarli EI, Langer T. 2012. Mitochondrial quality control: A matter of life and death for neurons. *EMBO J* **31**: 1336–1349.
- Russell RC, Fang C, Guan KL. 2011. An emerging role for TOR signaling in mammalian tissue and stem cell physiology. *Development* **138**: 3343–3356.
- Sarbassov DD, Guertin DA, Ali SM, Sabatini DM. 2005. Phosphorylation and regulation of Akt/PKB by the rictor-mTOR complex. *Science* **307**: 1098–1101.
- Shiba-Fukushima K, Imai Y, Yoshida S, Ishihama Y, Kanao T, Sato S, Hattori N. 2012. PINK1-mediated phosphorylation of the Parkin ubiquitin-like domain primes mitochondrial translocation of Parkin and regulates mitophagy. *Sci Rep* **2**: 1002.
- Ulatanir SK, Hertz NT, Li G, Ge WP, Burlingame AL, Pleasure SJ, Shokat KM, Jan LY, Jan YN. 2012. Chemical genetic identification of NDR1/2 kinase substrates AAK1 and Rabin8 uncovers their roles in dendrite arborization and spine development. *Neuron* **73**: 1127–1142.
- Valente EM, Abou-Sleiman PM, Caputo V, Muqit MM, Harvey K, Gispert S, Ali Z, Del Turco D, Bentivoglio AR, Healy DG, et al. 2004. Hereditary early-onset Parkinson's disease caused by mutations in PINK1. *Science* **304**: 1158–1160.
- Vilain S, Esposito G, Haddad D, Schaap O, Dobrev MP, Vos M, Van Meensel S, Morais VA, De Strooper B, Verstreken P. 2012. The yeast complex I equivalent NADH dehydrogenase rescues pink1 mutants. *PLoS Genet* **8**: e1002456.
- Wang X, Winter D, Ashrafi G, Schlehe J, Wong YL, Selkoe D, Rice S, Steen J, Lavoie MJ, Schwarz TL. 2011. PINK1 and Parkin target miro for phosphorylation and degradation to arrest mitochondrial motility. *Cell* **147**: 893–906.
- Wullschlegel S, Loewith R, Hall MN. 2006. TOR signaling in growth and metabolism. *Cell* **124**: 471–484.
- Yang Y, Gehrke S, Imai Y, Huang Z, Ouyang Y, Wang JW, Yang L, Beal MF, Vogel H, Lu B. 2006. Mitochondrial pathology and muscle and dopaminergic neuron degeneration caused by inactivation of *Drosophila* Pink1 is rescued by Parkin. *Proc Natl Acad Sci* **103**: 10793–10798.
- Yang Y, Ouyang Y, Yang L, Beal MF, McQuibban A, Vogel H, Lu B. 2008. Pink1 regulates mitochondrial dynamics through interaction with the fission/fusion machinery. *Proc Natl Acad Sci* **105**: 7070–7075.
- Ziviani E, Tao RN, Whitworth AJ. 2010. *Drosophila* parkin requires PINK1 for mitochondrial translocation and ubiquitinates Mitofusin. *Proc Natl Acad Sci* **107**: 5018–5023.
- Zoncu R, Efeyan A, Sabatini DM. 2011. mTOR: From growth signal integration to cancer, diabetes and ageing. *Nat Rev Mol Cell Biol* **12**: 21–35.



**Editor's comment:** By systematically obtaining information from the charts of an impressively large number of patients with Parkinson's disease (PD) followed in an outpatient neurology clinic, Yoritaka and colleagues have provided us a treasure trove of information and data that will serve as a valuable reference point for both clinicians and researchers. In addition to useful demographic and treatment information, they also have accumulated very interesting data on a number of aspects of PD that often receive scant attention, such as the frequency of camptocormia and pneumonia in PD patients.

**Ronald F. Pfeiffer**, Editor-in-Chief Department of Neurology, University of Tennessee HSC, 875 Monroe Avenue, Memphis, TN 38163, USA

## Motor and non-motor symptoms of 1453 patients with Parkinson's disease: Prevalence and risks



Asako Yoritaka<sup>a,b,\*</sup>, Yasushi Shimo<sup>a</sup>, Masashi Takanashi<sup>a</sup>, Jiro Fukae<sup>a,c</sup>, Taku Hatano<sup>a</sup>, Toshiki Nakahara<sup>a</sup>, Nobukazu Miyamoto<sup>a</sup>, Takao Urabe<sup>a,d</sup>, Hideo Mori<sup>a,b</sup>, Nobutaka Hattori<sup>a</sup>

<sup>a</sup> Department of Neurology, Juntendo University School of Medicine, Japan

<sup>b</sup> Department of Neurology, Juntendo University Koshigaya Hospital, Japan

<sup>c</sup> Department of Neurology, Fukuoka University Hospital, Japan

<sup>d</sup> Department of Neurology, Juntendo University Urayasu Hospital, Japan

### ARTICLE INFO

#### Article history:

Received 2 January 2013

Received in revised form

22 March 2013

Accepted 2 April 2013

#### Keywords:

Parkinson's disease  
Natural history studies  
Wearing-off  
Camptocormia  
Psychosis

### ABSTRACT

**Purpose:** We examined the prevalence and risk of clinical symptoms in a large number of Japanese patients with Parkinson's disease (PD) ( $n = 1453$ ; 650 males).

**Methods:** Events were analyzed using Kaplan–Meier survival curves, logistic regression, and Cox proportional-hazards models.

**Results:** The mean age (SD) was 67.7 (10.0), age of onset was 58.0 (11.5), and disease duration was 9.7 (6.6) years. The mean modified Hoehn and Yahr stage was 2.8 (1.2). Most patients (88.9%) received levodopa (547.7 (257.6) mg/day). A large proportion (81.3%) received dopamine agonists (136.2 (140.7) mg/day). About 23.4% received pain treatment 6.9 (5.1) years after the onset; females ( $p < 0.05$ ) and patients with late-onset PD ( $\geq 60$  years,  $p < 0.001$ ) were more likely to be affected. About 44.7% of patients had wearing-off 7.5 (4.7) years after the onset, and it was more common in females ( $p < 0.001$ ) and patients with early-onset PD ( $p < 0.001$ ). Camptocormia was found in 9.5% of patients 8.1 (6.2) years after the onset, and it was more common in females ( $p < 0.05$ ) and patients with late-onset PD ( $p < 0.05$ ). About 28.6% of patients developed psychosis 9.0 (5.4) years after the onset, and it was more likely to occur in patients with late-onset PD ( $p < 0.001$ ). Late-onset PD and cerebrovascular disease were also associated with increased risk of pneumonia.

**Conclusions:** Considering that very few studies have assessed numerous clinical symptoms in the same report, these data provide a useful reference for the clinical course of PD.

© 2013 Elsevier Ltd. All rights reserved.

## 1. Introduction

Parkinson's disease (PD) is the second most common neurodegenerative disorder after Alzheimer's disease. Dopamine

replacement with levodopa or dopamine agonists (DA) results in marked improvement of motor symptoms and alleviation of disability; these treatments have also improved patient survival [1,2]. However, levodopa use is also associated with the development of motor complications that substantially contribute to disability in patients with advanced PD. Various motor and non-motor symptoms (NMS) and side effects of anti-parkinsonian drugs limit the medication dose and the ability to prescribe other drugs. Here, we have described the prevalence and risk

\* Corresponding author. Department of Neurology, Juntendo University Koshigaya Hospital, Fukuroyama 560, Saitama 343-0032, Japan. Tel.: +81 48 975 0321; fax: +81 48 975 0346.

E-mail addresses: [ayori@juntendo.ac.jp](mailto:ayori@juntendo.ac.jp), [yyykoro@yahoo.co.jp](mailto:yyykoro@yahoo.co.jp) (A. Yoritaka).

**Table 1**  
Baseline demographic and clinical characteristics of patients with Parkinson's disease.

Variable	Category	n or mean	SD	Median
Total		1453		
Age		67.7	10.0	68.5
Age at onset		58.0	11.5	59.3
Sex	Male	650 (44.7%)		
	Female	803 (55.3%)		
Disease duration	Mean	9.7	6.6	8.5
Hoehn and Yahr stage on	First visit	10 (0.7%)	Enrollment	
	0	48 (3.3%)	48 (3.3%)	
	0.5 and 1.0	241 (16.6%)	101 (7.0%)	
	1.5 and 2.0	685 (47.1%)	428 (29.5%)	
	2.5 and 3.0	414 (28.5%)	438 (30.1%)	
	4	68 (4.7%)	294 (20.2%)	
	5	10 (0.7%)	99 (6.8%)	
	Not described	25 (1.7%)	45 (3.1%)	
Hypertension		258 (17.8%)		
Dyslipidemia		174 (12.0%)		
Diabetes mellitus		79 (5.4%)		
Cerebral vessel disease		86 (5.9%)		
Malignant tumor		87 (6.0%)		
Therapy in another hospital before our hospital		802 (55.2%)		
Anti-parkinsonian drugs				
Levodopa		1292 (88.9%)		
Duration from onset to start of treatment	Years	2.9	3.2	2.0
Daily dose at enrollment day	mg	547.7	257.6	600.0
Cumulative dose	g	1259.2	1190.0	933.4
Pramipexole		900 (61.9%)		
Duration from onset to start of treatment	Years	6.4	5.6	5.0
Daily dose (n = 900)	mg	2.1	2.6	1.7
Ropinirole		212 (14.6%)		
Duration from onset to start of treatment	Years	7.5	6.1	6.0
Daily dose (n = 212)	mg	7.5	4.7	3.3
Pergolide		414 (28.5%)		
Duration from onset to start of treatment	Years	4.9	4.9	3.5
Daily dose (n = 414)	mg	941.4	2.0	1.6
Cabergoline		405 (27.9%)		
Duration from onset to start of treatment	Years	4.9	5.2	3.3
Daily dose (n = 405)	mg	2.3	1.3	2.0
Bromocriptine		99 (6.8%)		
Duration from onset to start of treatment	Years	4.3	4.2	3.4
Daily dose (n = 99)	mg	16.2		7.5
Dopamine agonist		1182 (81.3%)		
Duration from onset to start of treatment	Years	4.0	4.4	2.6
Daily dose (n = 1453)	mg	136.2	140.7	120.0
Entacapone		314 (21.6%)		
Duration from onset to start of treatment	Years	10.3	5.8	9.3
Daily dose (n = 314)	mg	490.3	249.3	400.0
Trihexyphenidyl		561 (38.6%)		
Duration from onset to start of treatment	Years	4.0	4.0	2.7
Daily dose (n = 561)	mg	3.3	1.6	3.0
Amantadine		598 (41.2%)		
Duration from onset to start of treatment	Years	5.6	5.8	3.9
Daily dose (n = 598)	mg	166.0	63.6	150.0
Zonisamide		98 (6.7%)		
Duration from onset to start of treatment	Years	9.9	7.2	8.2
Daily dose (n = 98)	mg	47.3	34.9	25.0
Droxidopa		134 (9.2%)		
Duration from onset to start of treatment	Years	7.0	5.1	5.9
Daily dose (n = 134)	mg	380.6	178.7	300.0
Selegiline		620 (42.7%)		
Duration from onset to start of treatment	Years	6.7	5.0	5.6
Daily dose (n = 620)	mg	7.2	6.0	5.0

of clinical symptoms in a large number of Japanese patients with PD.

## 2. Patients and methods

Between January and June 2010, we retrospectively reviewed the charts of patients who had visited our outpatient neurology clinic at Juntendo Hospital in Tokyo, and had been diagnosed with PD by a board-certified neurologist. Diagnoses were based on the UK Brain Bank diagnostic criteria for PD [3], and patients with dementia with Lewy bodies [4], progressive supranuclear palsy, corticobasal

degeneration, vascular parkinsonism, and other forms of parkinsonism were excluded. Hospital charts were systematically reviewed by A.Y. This study was approved by the Juntendo Hospital institutional ethics committee, and informed consent was obtained.

The following data were collected from patients: sex; date of birth, first visit, and onset; initial symptoms, side of initial symptoms, order of medications taken from the time of initial medication, approximate date of start or stop of each medication, and modified Hoehn and Yahr (H & Y) stage for the initial and final evaluations; and dates of important events (pain, wearing-off, camptocormia, sleep attack, orthostatic hypotension, psychosis, electrical convulsive therapy [ECT] for severe psychosis, neuroleptic malignant syndrome, pneumonia, and tube feeding).

“Onset” was defined as the date of appearance of the first symptoms of parkinsonism (bradykinesia, rest tremor, and/or rigidity). “Pain” was defined as pain that required treatment, including pain related to wearing-off and excluding pain related to bone fracture, myocardial infarction, respiratory disease, and abdominal disease. “Camptocormia” was defined as marked anterior flexion of the thoracolumbar spine in the recumbent position without evidence of fixed kyphosis. “Sleep Attack” was an acute and irresistible episode of sleep occurring without warning signs [5]. “Orthostatic hypotension” was defined as a greater than 20 mmHg decrease in systolic pressure. “Psychosis” included reports of illusion, false sense of presence, hallucinations, or delusions that continued or recurred for at least 1 month [6]. Diagnosis of “neuroleptic malignant syndrome” was based on Levenson’s criteria [7]. Other NMS like depression, cognition, apathy, and excessive daytime sleepiness were not selected, because their onset was not clear, and the patients were not regularly examined using tools like the NMS questionnaire (NMSQuest) [8], Scale for Outcomes in Parkinson’s Disease-Psychiatric Complications (SCOPA-PC) [9], or SCOPA-Cognition (SCOPA-COG) [10]. NMS in early PD like REM sleep behavior disorder (RBD), olfactory dysfunctions, or constipation were not analyzed.

The daily levodopa equivalent dose was calculated on the basis of the following equivalences: 100 mg standard levodopa = 10 mg bromocriptine = 1 mg pergolide = 5 mg ropinirole = 1 mg pramipexole [11].

2.1. Statistical analyses

SAS (ver. 9.1.3; SAS Institute Inc., Cary, NC, USA) and SPSS (ver. 16.1; SPSS Inc., Chicago, IL, USA) were used for statistical analyses. The data are presented as mean (standard deviation [SD]) values for age, age at onset, H & Y stage of the “on” phase, daily dose of drugs, and duration from the onset of PD for important events. H & Y stages without parkinsonism symptoms in the “on” phase were considered as “0”. Point prevalences were calculated, and Kaplan–Meier (K–M) time-to-event curves and log-rank tests were used to estimate the absolute risk of each event. The factors chosen were as follows: onset age (early onset < 60 years or late onset ≥ 60 years), sex, hypertension (HT), diabetes mellitus (DM), dyslipidemia (DL), cerebrovascular disease (CVD), and malignant tumor. These were selected because they are the most frequently seen diseases in the Japanese. Logistic regression was performed to calculate odds ratios (ORs) with 95% confidence intervals (CIs) for each event. Cox

proportional-hazard modeling was used to calculate hazard ratios (HRs) and 95% CIs for differences among subgroups embedded into the following variables: age at onset, sex, order of drugs (levodopa or other anti-parkinsonism drugs), and duration to the start of drugs (levodopa, other drugs, or all anti-parkinsonism drugs). Proportional hazards were assessed with graph log–log plots. Statistical tests were two-sided, and the significance level was set at  $p < 0.05$ .

3. Results

We evaluated 1453 patients with PD (650 males) (Table 1). Their mean age (SD) was 67.7 (10.0), age of onset was 58.1 (11.5), and disease duration was 9.7 (6.6) years. The mean follow-up at our hospital was 5.9 (5.7) years. Age and age at onset were 67.2 (10.2) and 57.5 (11.8) years, respectively, for males and 68.3 (9.6) and 58.6 (11.2) years, respectively, for females. The mean H & Y stages were 2.2 (0.8) at the first visit and 2.8 (1.2) at the final evaluation. Patients with H & Y stages of 0, I (0.5 and 1.0), II (1.5 and 2.0), III (2.5 and 3.0), IV (4.0), V (5), and unknown (not described) were 3.3%, 7.0%, 29.5%, 30.1%, 20.2%, 6.8%, and 1.7%, respectively. The percentages of patients with PD who also had HT, DL, DM, CVD, and malignant tumor were 17.8%, 12.0%, 5.4%, 5.9%, and 6.0%, respectively.

Most patients (1292, 88.9%) received levodopa, and the average daily dose at enrollment was 547.7 (257.6) mg/day. The average levodopa doses for patients with H & Y stages of 0, I, II, III, IV, and V were 504.2 (252.8) mg, 498.0 (283.5) mg, 511.5 (304.2) mg, 484.9 (303.8) mg, 461.9 (283.4) mg, and 475.3 (270.1) mg, respectively (including unmedicated patients). In total, 1182 patients (81.3%) also received DAs; the average equivalent dose at enrollment was 136.2 (140.7) mg/day. The equivalent DA doses were 134.4 (142.4) mg, 136.9 (138.1) mg, 136.6 (139.0) mg, 140.8 (142.3) mg, 129.5

Table 2  
Kaplan–Meier survival of events in the patients with Parkinson’s disease.

Factors	Category	N	n (%)	Disease duration and prevalence: Kaplan–Meier (%)						Log-rank test
				2nd year	4th year	6th year	8th year	10th year	12th year	
				<i>n</i>						
				1356	1162	965	760	583	426	
Pain	Total	1453	340 (23.4)	3.2%	7.1%	13.2%	19.8%	25.0%	30.2%	–
Age of onset	<60	711	178 (25.0)	1.6%	4.4%	9.8%	15.1%	21.1%	25.5%	$P < 0.001^{***}$
	≥60	742	162 (21.8)	4.8%	9.9%	16.9%	25.7%	29.4%	37.0%	
Sex	Male	650	133 (20.5)	2.5%	6.2%	11.7%	17.6%	21.0%	26.5%	$P = 0.018^*$
	Female	803	207 (25.8)	3.7%	7.9%	14.5%	21.6%	28.0%	33.1%	
Wearing-off	Total	1453	649 (44.7)	1.8%	9.9%	22.7%	40.5%	50.9%	61.8%	–
Sex	Male	650	253 (38.9)	1.3%	8.5%	18.6%	34.5%	40.9%	52.9%	$P < 0.001^{***}$
	Female	803	396 (49.3)	2.2%	11.1%	26.0%	45.4%	58.8%	68.7%	
Camptocormia	Total	1453	138 (9.5)	0.7%	2.7%	5.2%	7.5%	9.3%	11.8%	–
Age of onset	<60	711	80 (11.3)	0.7%	1.5%	3.5%	5.5%	7.0%	10.0%	$P = 0.034^*$
	≥60	742	58 (7.8)	0.7%	4.1%	7.2%	9.9%	12.1%	13.4%	
Sex	Male	650	47 (7.2)	0.2%	1.6%	3.9%	6.4%	7.5%	9.1%	$P = 0.010^*$
	Female	803	91 (11.3)	1.1%	3.6%	6.3%	8.5%	10.7%	13.9%	
Sleep attack	Total	1453	65 (4.5)	0.4%	1.3%	2.4%	4.4%	6.7%	10.5%	–
Orthostatic hypotension	Total	1453	95 (6.5)	0.5%	1.6%	3.0%	4.8%	6.0%	8.3%	–
Age of onset	<60	711	45 (6.3)	0.1%	0.4%	1.4%	2.5%	3.0%	5.3%	$P < 0.001^{***}$
	≥60	742	50 (6.7)	0.8%	2.8%	4.9%	7.9%	10.5%	12.8%	
Hypertension	–	1195	88 (7.4)	0.5%	1.8%	3.4%	5.5%	6.8%	9.5%	$P = 0.005^{**}$
	+	258	7 (2.7)	0.4%	0.9%	0.9%	1.5%	2.3%	2.3%	
Psychosis	Total	1453	416 (28.6)	1.7%	5.8%	11.1%	18.0%	25.6%	33.8%	–
Age of onset	<60	711	207 (29.1)	0.7%	2.5%	5.8%	11.2%	16.0%	22.1%	$P < 0.001^{***}$
	≥60	742	209 (28.2)	2.7%	9.4%	17.2%	26.6%	39.8%	53.9%	
Malignant syndrome	Total	1453	32 (2.2)	0.1%	0.2%	0.3%	1.1%	2.2%	2.8%	–
Diabetes mellitus	–	1374	27 (2.0)	0.1%	0.2%	0.3%	1.1%	1.7%	2.4%	$P = 0.032^*$
	+	79	5 (6.3)	0.0%	0.0%	0.0%	2.0%	9.0%	9.0%	
Pneumonia	Total	1453	63 (4.3)	0.1%	0.2%	0.7%	1.5%	2.8%	3.3%	–
Age of onset	<60	711	27 (3.8)	0.0%	0.0%	0.3%	0.3%	0.6%	0.8%	$P < 0.001^{***}$
	≥60	742	36 (4.9)	0.1%	0.5%	1.1%	3.1%	6.6%	7.9%	
Cerebrovascular disease	–	1367	51 (3.7)	0.1%	0.2%	0.5%	1.0%	2.1%	2.7%	$P < 0.001^{***}$
	+	86	12 (14.0)	0.0%	1.3%	4.1%	7.6%	11.7%	11.7%	

All events were analyzed with all factors. The factors were designed as follows, onset age, sex, hypertension, diabetes mellitus, dyslipidemia, cerebrovascular disease, and malignant tumor. Table indicates only factors with significant differences. \*:  $p < 0.05$ , \*\*:  $p < 0.01$ , \*\*\*:  $p < 0.001$ .

**Table 3**  
Logistic regression of the events in patients with Parkinson's disease.

Factors	Statistical analysis	Age at onset	Age	Sex (female)	Disease duration	Modified Hoehn and Yahr stage	Daily levodopa (mg)	Duration to start of levodopa	Duration start of the drugs except levodopa	First start of the drugs	Hypertension
Pain	Odds ratio	0.85	1.18	1.42	0.83	1.00	1.00	0.10	0.96	0.83	
	CI	0.66–1.08	0.92–1.51	1.08–1.87	0.65–1.06	0.87–1.15	1.00–1.00	1.00–1.00	0.92–1.01	0.60–1.16	NE
	<i>p</i>	0.177	0.191	0.013*	0.128	0.996	<0.001***	0.099	0.090	0.283	
Wearing-off	Odds ratio	0.97	0.97	2.13	1.00	0.93	1.00	0.99	0.99	1.28	
	CI	0.75–1.27	0.75–1.23	1.61–280	0.77–1.29	0.82–1.07	1.00–1.00	1.00–1.00	0.93–1.04	0.91–1.79	NE
	<i>p</i>	0.840	0.815	<0.001***	0.989	0.316	<0.001***	<0.001***	0.592	0.156	
Camptocormia	Odds ratio	0.88	1.12	1.56	0.87	1.37	1.00	1.00	0.95	1.00	
	CI	0.68–1.14	0.86–1.45	1.07–2.28	0.68–1.12	1.13–1.66	1.00–1.00	1.00–1.00	0.88–1.02	0.63–1.57	NE
	<i>p</i>	0.319	0.403	0.022*	0.278	0.002**	0.113	0.681	0.144	0.860	
Sleep attack	Odds ratio	0.98	1.00	0.60	NE	1.01	1.00	0.93	0.88	1.21	NE
	CI	0.93–1.03	0.95–1.06	0.36–1.00		0.78–1.30	0.99–1.00	0.78–1.11	0.76–1.02	0.93–1.58	
	<i>p</i>	0.980	0.970	0.048*		0.967	0.889	0.434	0.101	0.151	
Orthostatic hypotension	Odds ratio	0.86	1.19	0.95	0.82	1.32	1.00	1.00	1.03	1.25	4.47
	CI	0.66–1.11	0.91–1.54	0.60–1.51	0.64–1.05	1.03–1.69	1.00–1.00	1.00–1.00	0.97–1.09	0.71–2.21	1.01–19.75
	<i>p</i>	0.235	0.200	0.826	0.117	0.028*	0.190	0.016*	0.386	0.433	0.048*
Psychosis	Odds ratio	0.98	1.06	1.20	1.01	1.49	1.00	1.04	0.94	0.68	
	CI	0.91–1.05	0.98–1.14	0.79–1.81	0.94–1.08	1.21–1.88	1.00–1.00	0.96–1.13	0.88–1.00	0.41–1.14	NE
	<i>p</i>	0.505	0.136	0.401	0.845	<0.001***	<0.001***	0.360	0.061	0.144	

CI: confidence interval, \*:  $p < 0.05$ , \*\*:  $p < 0.01$ , \*\*\*:  $p < 0.001$ , NE: not examined.

(134.2) mg, and 131.4 (156.3) mg for H & Y stages 0, I, II, III, IV, and V, respectively (including unmedicated patients). Equivalent DA doses in H & Y stages I and II were not significantly different between patients with wearing-off (159.8 (156.0) mg) and those without wearing-off (131.6 (137.0) mg). The average levodopa dose for H & Y stage I and II patients was 538.8 (214.6) mg with wearing-off and 278.0 (247.4) mg without wearing-off; this difference was statistically significant ( $p < 0.001$ ). H & Y stage I and II patients with psychosis were on higher doses of levodopa (535.9 (220.2) mg) compared to patients without psychosis (336.9 (263.5) mg) ( $p < 0.001$ ). The average DA dose was 119.5 (151.6) mg in patients with psychosis and 146.9 (143.3) mg in those without ( $p > 0.05$ ).

The onset of events was significantly ( $p < 0.001$ ) earlier in patients with late onset than in those with early onset (Additional

Table 1S). The prevalence and mean duration of each symptom from onset of PD are shown in Additional Fig. 1. The data obtained from K–M curves, logistic regression, and Cox HRs are shown in Tables 2–4, respectively.

### 3.1. Pain

About 23.4% of patients had pain at a mean duration of 6.94 (5.12) years from PD onset. In the twelfth year, 37.0% of late-onset and 25.5% of early-onset patients reported pain ( $p < 0.001$ ); there was a statistically significant sex difference ( $p < 0.05$ ). Logistic regression showed that the pain OR was 1.42 (95% CI, 1.08–1.87;  $p < 0.05$ ) for females. Cox modeling yielded an HR of 1.26 (95% CI, 1.08–1.58;  $p < 0.05$ ) for females and 1.02 (95% CI, 1.01–1.03;  $p < 0.001$ ) for age at onset.

**Table 4**  
Cox proportional hazards models for clinical events in patients with Parkinson's disease.

Events	Variables	Age at onset	Sex (female)	Duration to start of levodopa	Duration to start of the drugs except levodopa	First start of the drugs	No hyper-tension	Diabetes mellitus+	Cerebro-vascular disease+
Pain	HR	1.02	1.26	0.93	0.95	1.06			
	95%CI	1.01–1.03	1.08–1.58	0.86–1.00	0.91–0.99	0.79–1.41	NE	NE	NE
	<i>p</i>	<0.001***	0.043*	0.059	0.01*	0.701			
Wearing off	HR	0.99	1.46	0.89	0.97	0.86			
	95%CI	0.98–0.99	1.24–1.71	0.84–0.94	0.95–0.99	0.70–1.04	NE	NE	NE
	<i>p</i>	<0.001***	<0.001***	<0.001***	0.006**	0.123			
Camptocormia	HR	1.02	1.46	1.01	0.94	1.08			
	95%CI	1.01–1.04	1.03–2.08	0.90–1.12	0.88–1.00	0.70–1.68	NE	NE	NE
	<i>p</i>	0.012*	0.033*	0.909	0.053	0.723			
Sleep attack	HR	1.02	0.55	0.89	0.85	1.20			
	95%CI	0.99–1.05	0.33–0.90	0.75–1.05	0.74–0.98	0.93–1.53	NE	NE	NE
	<i>p</i>	0.085	0.017*	0.152	0.021*	0.160			
Orthostatic hypotension	HR	1.04	0.87	0.93	1.03	0.94	1.63		
	95%CI	1.02–1.06	0.57–1.34	0.79–1.09	0.98–1.08	0.53–1.66	0.97–2.74	NE	NE
	<i>p</i>	0.001**	0.532	0.345	0.332	0.834	0.063		
Psychosis	HR	1.05	1.04	0.99	0.97	1.16			
	95%CI	1.04–1.07	0.85–1.26	0.93–1.06	0.94–1.01	0.90–1.51	NE	NE	NE
	<i>p</i>	<0.001***	0.714	0.781	0.096	0.253			
Malignant syndrome	HR	1.05	0.73	0.94	1.01	2.05		2.47	
	95%CI	0.99–1.06	0.35–1.53	0.74–1.21	0.93–1.09	0.70–6.01	NE	0.87–6.97	NE
	<i>p</i>	0.176	0.404	0.646	0.883	0.189		0.088	
Pneumonia	HR	1.13	0.63	1.07	0.99	2.00			1.98
	95%CI	1.09–1.16	0.83–1.06	0.91–1.26	0.93–1.05	0.93–4.29	NE	NE	1.03–3.80
	<i>p</i>	<0.001***	0.083	0.435	0.771	0.076			0.041*

HR: hazard rate, CI: confidence interval, \*:  $p < 0.05$ , \*\*:  $p < 0.01$ , \*\*\*:  $p < 0.001$ , NE: not examined.

### 3.2. Wearing-off

About 44.7% of patients experienced wearing-off an average of 7.52 (4.66) years after PD onset. The prevalence of dyskinesia was 27.1%, and all of these patients had wearing-off. Wearing-off was more common in females ( $p < 0.001$ ); 58.8% of female and 40.9% of male patients had experienced it by the tenth year. Logistic regression analysis revealed a significantly higher OR for female sex, daily dose of levodopa, and disease duration to the start of levodopa. HRs were 1.46 (95% CI, 1.24–1.71;  $p < 0.001$ ) for female sex, 0.99 (95% CI, 0.98–0.99;  $p < 0.001$ ) for age at onset, 0.89 (95% CI, 0.84–0.94;  $p < 0.001$ ) for disease duration to the start of levodopa, and 0.97 (95% CI, 0.95–0.99;  $p < 0.01$ ) for the duration to the start of other drugs.

### 3.3. Camptocormia

Camptocormia was found in 9.5% of patients an average of 8.05 (6.16) years after PD onset. Prevalence was higher in late-onset patients than in early-onset patients ( $p < 0.05$ ), and more females developed the symptom ( $p < 0.01$ ). Logistic regression analysis revealed significantly higher ORs for female sex and higher H & Y stages. HRs were 1.02 (95% CI, 1.01–1.04;  $p < 0.05$ ) for age at onset and 1.46 (95% CI, 1.03–2.08;  $p < 0.05$ ) for female sex. In 34 patients, we stopped pramipexole and their camptocormia improved; therefore, we also assessed camptocormia risk in patients who did or did not receive non-ergot DAs. Among patients who received pramipexole, females showed a higher prevalence of camptocormia (7.7% in the second year and 14.8% in the fourth year), and males had lower prevalence in the early stage of disease (3.8% in the second year, 6.5% in the fourth year) ( $p < 0.01$ ). The HRs for patients on pramipexole were 1.82 (95% CI, 1.21–2.72;  $p < 0.001$ ) for female sex and 0.67 (95% CI, 0.54–0.83;  $p < 0.001$ ) for disease duration. For those who experienced camptocormia without non-ergot DAs, no differences were observed for age at onset, sex, or accompanying disease.

### 3.4. Sleep attack

An average of 8.50 (6.52) years from PD onset, 4.5% of patients had sleep attack without warning signs. Daily DA doses were not correlated to the prevalence of sleep attack. Logistic regression analysis revealed significantly higher ORs for male sex. HRs were 0.60 (95% CI, 0.36–1.00;  $p < 0.05$ ) for female sex.

### 3.5. Orthostatic hypotension

An average of 8.83 (6.04) years from PD onset, 6.5% of patients developed orthostatic hypotension that required treatment. Notably, 12.8% of late-onset patients had orthostatic hypotension by the twelfth year compared to just 5.3% of early-onset patients. Logistic regression revealed that the OR was significantly higher for higher H & Y stages and patients without hypertension. The HR was 1.039 (95% CI, 1.02–1.06;  $p < 0.01$ ) for age at onset.

### 3.6. Psychosis

About 28.6% of patients had symptoms of psychosis an average of 9.03 (5.38) years after PD onset. Interestingly, 53.9% of late-onset patients and 22.1% of early-onset patients had experienced symptoms of psychosis by the twelfth year ( $p < 0.001$ ). Logistic regression tests revealed that the OR was significantly larger for higher H & Y stages and greater levodopa doses. The HR was 1.05 (95% CI, 1.04–1.07;  $p < 0.001$ ) for age of onset.

Seventeen patients underwent ECT for the treatment of psychotic symptoms that were refractory to medication. ECT took place an average of 8.24 (6.07) years after PD onset. The prevalence rate for ECT was 1.8% in the twelfth year. More patients with DM than without DM (3.8% vs. 1.0%) received ECT ( $p < 0.05$ ). Logistic regression revealed no OR effects for ECT (data not shown).

### 3.7. Neuroleptic malignant syndrome

About 2.2% of patients developed neuroleptic malignant syndrome an average of 11.44 (7.79) years after PD onset. Among patients with DM, 9.0% developed malignant syndrome, whereas only 1.7% of patients without DM had experienced malignant syndrome by the tenth year ( $p < 0.05$ ). Logistic regression and HR assessments did not reveal any risk factors that predisposed patients to developing malignant syndrome.

### 3.8. Pneumonia

About 4.3% of patients developed pneumonia, which occurred an average of 13.87 (8.04) years after PD onset. Late-onset patients ( $p < 0.001$ ) and those with CVD ( $p < 0.001$ ) were more likely to develop pneumonia. The HR was 1.13 (95% CI, 1.09–1.16;  $p < 0.001$ ) for age at onset and 1.98 (95% CI, 1.03–3.80;  $p < 0.05$ ) for CVD. Tube feeding was necessary in 2.1% of patients after an average of 16.03 (9.36) years after PD onset. Tube feeding prevalence rates were 0.1%, and 1.8% in the sixth and twelfth years, respectively.

## 4. Discussion

In Western countries, the prevalence and incidence of PD are greater in males than in females [12,13]. In our study, there were more female patients, which is similar to what was previously reported in a Japanese PD study (male:female, 1:1.2–1.7) [14,15]. In this retrospective non-interventional study, we assessed symptom prevalence and duration in a large cohort of Japanese patients with PD. The duration to the onset of events, except for malignant syndrome, in the early-onset group was 1.5–2 times greater than that in the late-onset group.

The questionnaire-based study by Chaudhuri et al. [16] revealed no differences in pain rate (27% for patients with PD vs. 30.2% for age matched-controls). Other studies have described higher pain rates in patients with PD [17,18]; however, the studies utilized different pain scales. We found that females and late-onset patients had increased pain rates, but other reports have stated that younger age at onset [17] and female sex [19–21] were risk factors for pain.

Female patients were more likely to experience wearing-off, and the average female daily dose of levodopa was higher (11.5 (5.8) mg/kg compared to 8.8 (3.9) mg/kg for males; Fisher's test,  $p < 0.01$ ). The DATATOP clinical trial showed that more females developed dyskinesia and that this was likely due to the higher amount of levodopa ( $p < 0.01$ ) [22]. In our study, younger age at onset was a risk for wearing-off. Which drug was prescribed first (levodopa or other drugs) did not affect wearing-off. A prospective study reported that motor complication prevalence was not significantly different between patients initially treated with levodopa and those first treated with DA [23–25]. Although there were no statistical differences, the time without motor complications was longer in the group initially treated with DA; however, these patients often experienced sleepiness, edema, and hallucinations [23–25]. In our 2002 study, the prevalence of wearing-off was 21.3% at the fifth year and 59.4% at the tenth year

from PD onset [15], which was slightly higher than what we found here. In the interim between the studies, new anti-parkinsonian drugs were marketed in Japan, including pramipexole (2004), ropinirole (2006), entacapone (2007), and zonisamide (2009). The availability of these drugs may have prolonged wearing-off onset because we could select from different DAs.

The prevalence of camptocormia and duration from PD onset to camptocormia in our study were nearly identical to those previously described [26,27]. We found that female sex, older age at onset, and disease severity were risk factors for camptocormia. In our patient population, camptocormia was more severe during walking or standing and tended to increase with fatigue and decrease when non-ergot drug use was ceased. Camptocormia was considered to be axial dystonia [28] rather than a myopathic change [26,27]. Levodopa [29] or pramipexole [30] induced or worsened camptocormia in some cases, but they may also have beneficial effects in cases in which it is due to PD. We investigated the risk of camptocormia in patients with PD receiving non-ergot DAs.

Sleep attack and excessive daytime sleepiness were more common in males [31]. Disease duration, DA therapy, excessive daytime sleepiness [32] and RBD [33] were risks of sleep attack. Varying frequencies of sleep attack (0–43%) have been reported [34].

A previous report showed that 60% of patients developed psychosis during a 12-year study period [35]. The analysis revealed that the risk of psychosis (mainly hallucinations) increased in patients with older age at onset and greater disease severity. In other studies, older age [36] and longer disease duration [37,38] were associated with psychosis, and disease severity was linked to the presence of hallucinations [38]. Moreover, hallucinations were more frequent among patients with early PD treated with DA compared with those who received placebo or levodopa [39]. In our study, patients with psychosis were treated with lower doses of DAs and higher doses of levodopa, and other drugs were stopped due to psychosis.

The risk of neuroleptic malignant syndrome has been previously associated with CVD, cerebral contusion, physical stress [40], infection, hot weather, and severe wearing-off [41]. In this study, CVD was not a risk factor. Many patients experienced dehydration or severe off-phases before neuroleptic malignant syndrome onset. Although malignant syndrome and dopamine agonist withdrawal syndrome [42] were both acute syndromes caused by a sudden change in dopaminergic stimulation, the risk factors for these syndromes were different.

Respiratory infection is one of the leading causes of death in patients with PD [15]. Patients with late-onset PD or CVD were at risk for developing pneumonia, and the mean duration of tube feeding was 2 years after the first episode of pneumonia.

The limitation of our retrospective study is that we did not include patients who died early. Furthermore, this study was a retrospective chart review study and certain treatment outcomes differed from those of previously reported controlled prospective studies.

NMSQuest studies [8,43] and the PRIAMO study [20] that used self-completed NMS questionnaire have reported that NMS were prevalent across all stages of PD disease. These studies broadly included a broad spectrum of NMS that patients may not be aware of as PD-related symptoms or clinicians ignored. However, until recently, NMS were known to clinicians treating PD and patients with PD, and many of the unrecognized NMS need treatment because these reduce the quality of life.

In conclusion, we investigated the duration and prevalence rates of various symptoms and complications in a large cohort of patients

with PD and determined that age and sex might predict the onset of some events. Moreover, the onset or duration of levodopa use might influence the onset of wearing-off, but the order of levodopa or other drugs did not predict symptoms.

#### Full financial disclosure

A. Yoritaka, Y. Shimo, M. Takanashi, J. Fukae, T. Hatano, T. Nakahara, N. Miyamoto, T. Urabe, and H. Mori report no disclosures. N. Hattori is a consultant for Boehringer Ingelheim, FP Pharmaceutical Company, Ohtsuka Pharmaceutical Company, Kyowa Hakko Kirin Pharmaceutical Company, GlaxoSmithKline, Novartis, Abbot, Hisamitsu, and Schering-Plough. He received personal compensation for attending advisory board meetings.

#### Study funding

None.

#### Author roles

1. Research Projects: A. Conception, Organization, B. Execution
2. Statistical Analysis: A. Design and Execution, Review and Critique
3. Manuscript: A. Writing of the First draft, B. Review and Critique.

A. Yoritaka: 1A, 1B, 2A, 3A, and 3B; Y. Shimo, M. Takanashi, J. Fukae, T. Hatano, T. Nakahara, N. Miyamoto, H. Mori, and N. Hattori: 1B; T. Urabe: 1B and 3B.

#### Acknowledgments

We thank Dr. K. Matsuoka, Juntendo Clinical Research Center, for advice regarding the statistical analysis. We thank Dr. A. Mori, Department of Neurology, Juntendo University School of Medicine, as well as the nurses and office workers for their assistance reviewing charts.

#### Appendix A. Supplementary data

Supplementary data related to this article can be found at <http://dx.doi.org/10.1016/j.parkreldis.2013.04.001>.

#### References

- [1] Ben-Shlomo Y, Marmot MG. Survival and cause of death in a cohort of patients with parkinsonism: possible clues to aetiology? *J Neurol Neurosurg Psychiatr* 1995;58:293–9.
- [2] Diem-Zangerl A, Seppi K, Wenning GK, Trinkla E, Ransmayr G, Oberaigner W, et al. Mortality in Parkinson's disease: a 20-year follow-up study. *Mov Disord* 2009;24:819–25.
- [3] Hughes AJ, Daniel SE, Kilford L, Lees AJ. Accuracy of clinical diagnosis of idiopathic Parkinson's disease: a clinico-pathological study of 100 cases. *J Neurol Neurosurg Psychiatr* 1992;55:181–4.
- [4] Mckeith IG, Dickson DW, Lowe J, Emre M, O'Brien JT, Feldman H, et al. Diagnosis and management of dementia with Lewy bodies: third report of DLB Consortium. *Neurology* 2005;65:1863–72.
- [5] Frucht S, Rogers JD, Greene PE, Gordon MF, Fahn S. Falling asleep at the wheel: motor vehicle mishaps in persons taking pramipexole and ropinirole. *Neurology* 1999;52:1908–10.
- [6] Ravina B, Marder K, Fernandez HH, Friedman JH, McDonald W, Murphy D, et al. Diagnostic criteria for psychosis in Parkinson's disease: report of an NINDS, NIMH work group. *Mov Disord* 2007;22:1061–8.
- [7] Levenson JL. Neuroleptic malignant syndrome. *Am J Psychiatry* 1985;142:1137–45.
- [8] Chaudhuri KR, Martinez-Martin P, Brown RG, Sethi K, Stocchi F, Odin P, et al. The metric properties of a novel non-motor symptoms scale for Parkinson's disease: results from an international pilot study. *Mov Disord* 2007;22:1901–11.

- [9] Visser M, Verbaan D, van Rooden SM, Stiggelbout AM, Marinus J, van Hilten JJ. Assessment of psychiatric complications in Parkinson's disease: the SCOPA-PC. *Mov Disord* 2007;22:2221–8.
- [10] Marinus J, Visser M, Verwey NA, Verhey FR, Middelkoop HA, Stiggelbout AM, et al. Assessment of cognition in Parkinson's disease. *Neurology* 2003;61:1222–8.
- [11] Chung SJ, Jeon SR, Kim SR, Sung YH, Lee MC. Bilateral effects of unilateral subthalamic nucleus deep brain stimulation in advanced Parkinson's disease. *Eur Neurol* 2006;56:127–32.
- [12] Wright Willis A, Evanoff BA, Lian M, Criswell SR, Racette BA. Geographic and ethnic variation in Parkinson disease: a population-based study of US Medicare beneficiaries. *Neuroepidemiology* 2010;34:143–51.
- [13] Linder J, Stenlund H, Forsgren L. Incidence of Parkinson's disease and parkinsonism in northern Sweden: a population-based study. *Mov Disord* 2010;25:341–8.
- [14] Harada H, Nishikawa S, Takahashi K. Epidemiology of Parkinson's disease in a Japanese city. *Arch Neurol* 1983;40:151–4.
- [15] Sato K, Hatano T, Yamashiro K, Kagohashi M, Nishioka K, Izawa N, et al. Prognosis of Parkinson's disease: time to stage III, IV, V, and to motor fluctuations. *Mov Disord* 2006;21:1384–95.
- [16] Chaudhuri KR, Martinez-Martin P, Schapira AH, Stocchi F, Sethi K, Odin P, et al. International multicenter pilot study of the first comprehensive self-completed nonmotor symptoms questionnaire for Parkinson's disease: the NMSQuest study. *Mov Disord* 2006;21:916–23.
- [17] Negre-Pages L, Regragui W, Bouhassira D, Grandjean H, Rascol O. Chronic pain in Parkinson's disease: the cross-sectional French DoPaMiP survey. *Mov Disord* 2008;23:1361–9.
- [18] Beiske AG, Loge JH, Ronningen A, Svensson E. Pain in Parkinson's disease: prevalence and characteristics. *Pain* 2009;141:173–7.
- [19] Scott B, Borgman A, Engler H, Johnels B, Aquilonius SM. Gender differences in Parkinson's disease symptom profile. *Acta Neurol Scand* 2000;102:37–43.
- [20] Barone P, Antonini A, Colosimo C, Marconi R, Morgante L, Avarello TP, et al. The PRIAMO study: a multicenter assessment of nonmotor symptoms and their impact on quality of life in Parkinson's disease. *Mov Disord* 2009;24:1641–9.
- [21] Martinez-Martin P, Pecurariu CF, Odin P, van Hilten JJ, Antonini A, Rojo-Abuin JM, et al. Gender-related differences in the burden of non-motor symptoms in Parkinson's disease. *J Neurol* 2012;259:1639–47.
- [22] Parkinson Study Group. Impact of deprenyl and tocopherol treatment on Parkinson's disease in DATATOP patients requiring levodopa. *Ann Neurol* 1996;39:37–45.
- [23] Hely MA, Morris JG, Reid WG, Trafficante R. Sydney multicenter study of Parkinson's disease: non-L-dopa-responsive problems dominate at 15 years. *Mov Disord* 2005;20:190–9.
- [24] Hauser RA, Rascol O, Korczyn AD, Jon Stoessl A, Watts RL, Poewe W, et al. Ten-year follow-up of Parkinson's disease patients randomized to initial therapy with ropinirole or levodopa. *Mov Disord* 2007;22:2409–17.
- [25] Katzenschlager R, Head J, Schrag A, Ben-Shlomo Y, Evans A, Lees AJ. Fourteen-year final report of the randomized PDRG-UK trial comparing three initial treatments in PD. *Neurology* 2008;71:474–80.
- [26] Margraf NG, Wrede A, Rohr A, Schulz-Schaeffer WJ, Raethjen J, Eymess A, et al. Camptocormia in idiopathic Parkinson's disease: a focal myopathy of the paravertebral muscles. *Mov Disord* 2010;25:542–51.
- [27] Spuler S, Krug H, Klein C, Medialdea IC, Jakob W, Ebersbach G, et al. Myopathy causing camptocormia in idiopathic Parkinson's disease: a multidisciplinary approach. *Mov Disord* 2010;25:552–9.
- [28] Fahn S. Current concept and classification of dystonia. *Adv Neurol* 1976;14:177–86.
- [29] Djaldetti R, Mosberg-Galili R, Sroka H, Merims D, Melamed E. Camptocormia (bent spine) in patients with Parkinson's disease—characterization and possible pathogenesis of an unusual phenomenon. *Mov Disord* 1999;14:443–7.
- [30] Nakayama Y, Miwa H. Drug-induced camptocormia: a lesson regarding vascular parkinsonism. *Intern Med* 2012;51:2843–4.
- [31] Ondo WG, Dat Vuong K, Khan H, Atassi F, Kwak C, Jankovic J. Daytime sleepiness and other sleep disorders in Parkinson's disease. *Neurology* 2001;57:1392–6.
- [32] Paus S, Brecht HM, Köster J, Seeger G, Klockgether T, Wüllner U. Sleep attacks, daytime sleepiness, and dopamine agonists in Parkinson's disease. *Mov Disord* 2003;18:659–67.
- [33] Yoritaka A, Ohizumi H, Tanaka S, Hattori N. Parkinson's disease with and without REM sleep behaviour disorder: are there any clinical differences? *Eur Neurol* 2009;61:164–70.
- [34] Ghorayeb I, Loundou A, Auquier P, Dauvilliers Y, Bioulac B, Tison F. A nationwide survey of excessive daytime sleepiness in Parkinson's disease in France. *Mov Disord* 2007;22:1567–72.
- [35] Forsaa EB, Larsen JP, Wentzel-Larsen T, Goetz CG, Stebbins GT, Aarsland D, et al. A 12-year population-based study of psychosis in Parkinson disease. *Arch Neurol* 2010;67:996–1001.
- [36] Sanchez-Ramos JR, Ortoll R, Paulson GW. Visual hallucinations associated with Parkinson disease. *Arch Neurol* 1996;53:1265–8.
- [37] Graham JM, Grunewald RA, Sagar HJ. Hallucinations in idiopathic Parkinson's disease. *J Neurol Neurosurg Psychiatr* 1997;63:434–40.
- [38] Barnes J, David AS. Visual hallucinations in Parkinson's disease: a review and phenomenological survey. *J Neurol Neurosurg Psychiatr* 2001;70:727–33.
- [39] Baker WL, Silver D, White CM, Kluger J, Aberle J, Patel AA, et al. Dopamine agonists in the treatment of early Parkinson's disease. *Parkinsonism Relat Disord* 2009;15:287–94.
- [40] Hashimoto T, Tokuda T, Hanyu N, Tabata K, Yanagisawa N. Withdrawal of levodopa and other risk factors for malignant syndrome in Parkinson's disease. *Parkinsonism Relat Disord* 2003;9:S25–30.
- [41] Takubo H, Harada T, Hashimoto T, Inaba Y, Kanazawa I, Kuno S, et al. A collaborative study on the malignant syndrome in Parkinson's disease and related disorders. *Parkinsonism Relat Disord* 2003;9:S31–41.
- [42] Cunnigton AL, White L, Hood K. Identification of possible risk factors for the development of dopamine agonist withdrawal syndrome in Parkinson's disease. *Parkinsonism Relat Disord* 2012;18:1051–2.
- [43] Chaudhuri KR, Prieto-Jurczynska C, Naidu Y, Mitra T, Frades-Payo B, Tluk S, et al. The nondeclaration of nonmotor symptoms of Parkinson's disease to health care professionals: an international study using the nonmotor symptoms questionnaire. *Mov Disord* 2010;25:704–9.



# Mutations in Fis1 disrupt orderly disposal of defective mitochondria

Qinfang Shen<sup>a</sup>, Koji Yamano<sup>b</sup>, Brian P. Head<sup>a,\*</sup>, Sumihiro Kawajiri<sup>a,c</sup>, Jesmine T. M. Cheung<sup>a</sup>, Chunxin Wang<sup>b</sup>, Jeong-Hoon Cho<sup>a,†</sup>, Nobutaka Hattori<sup>c</sup>, Richard J. Youle<sup>b</sup>, and Alexander M. van der Bliek<sup>a</sup>

<sup>a</sup>Department of Biological Chemistry, David Geffen School of Medicine at UCLA, Los Angeles, CA 90095;

<sup>b</sup>Biochemistry Section, Surgical Neurology Branch, National Institute of Neurological Disorders and Stroke, National Institutes of Health, Bethesda, MD 20892; <sup>c</sup>Department of Neurology, Juntendo University School of Medicine, Tokyo 113-8421, Japan

**ABSTRACT** Mitochondrial fission is mediated by the dynamin-related protein Drp1 in metazoans. Drp1 is recruited from the cytosol to mitochondria by the mitochondrial outer membrane protein Mff. A second mitochondrial outer membrane protein, named Fis1, was previously proposed as recruitment factor, but Fis1<sup>-/-</sup> cells have mild or no mitochondrial fission defects. Here we show that Fis1 is nevertheless part of the mitochondrial fission complex in metazoan cells. During the fission cycle, Drp1 first binds to Mff on the surface of mitochondria, followed by entry into a complex that includes Fis1 and endoplasmic reticulum (ER) proteins at the ER-mitochondrial interface. Mutations in Fis1 do not normally affect fission, but they can disrupt downstream degradation events when specific mitochondrial toxins are used to induce fission. The disruptions caused by mutations in Fis1 lead to an accumulation of large LC3 aggregates. We conclude that Fis1 can act in sequence with Mff at the ER-mitochondrial interface to couple stress-induced mitochondrial fission with downstream degradation processes.

## Monitoring Editor

Donald D. Newmeyer  
La Jolla Institute for Allergy  
and Immunology

Received: Sep 11, 2013

Revised: Oct 28, 2013

Accepted: Oct 30, 2013

## INTRODUCTION

Mitochondrial fission is mediated by dynamin-related proteins (Drp1 in metazoans and Dnm1 in yeast). These proteins are predominantly cytosolic, but a small fraction can assemble into spirals that wrap around the circumference of mitochondria and sever the membranes through constriction (Bleazard *et al.*, 1999; Labrousse *et al.*, 1999; Smirnova *et al.*, 2001; Ingerman *et al.*, 2005). Recruitment of Drp1 to mitochondria is mediated by proteins that are anchored in

the mitochondrial outer membrane. Mammalian cells have three structurally distinct classes of recruitment factors on their mitochondrial outer membranes: Fis1, Mff, and the two related proteins MiD49 and MiD51 (MIEF1; James *et al.*, 2003; Gandre-Babbe and van der Bliek, 2008; Otera *et al.*, 2010; Palmer *et al.*, 2011; Zhao *et al.*, 2011).

Fis1 was first discovered in yeast, in which it is the sole recruitment factor on the outer membrane (Mozdy *et al.*, 2000). This protein has two TPR motifs that bind to the yeast Drp1 homologue Dnm1 through adaptor proteins (Mdv1 and Caf4; Tieu and Nunnari, 2000; Griffin *et al.*, 2005; Koch *et al.*, 2005; Kobayashi *et al.*, 2007; Koirala *et al.*, 2010). Fis1 is present throughout the animal kingdom, but its functions in metazoans have been unclear. Fis1 can bind to human Drp1 *in vitro*, can promote fission when overexpressed, and has been implicated in a number of fission-dependent processes, such as apoptosis and autophagy (James *et al.*, 2003; Yoon *et al.*, 2003; Lee *et al.*, 2004; Jofuku *et al.*, 2005; Gomes and Scorrano, 2008; Twig *et al.*, 2008). However, mammalian Fis1<sup>-/-</sup> cells have mild or no fission defect (Otera *et al.*, 2010; Loson *et al.*, 2013), suggesting that Fis1 plays an ancillary role in the fission process.

This article was published online ahead of print in MBoc in Press (<http://www.molbiolcell.org/cgi/doi/10.1091/mbc.E13-09-0525>) on November 6, 2013.

Present addresses: \*Department of Molecular Genetics and Microbiology, Duke University Medical Center, Durham, NC 27710; †Division of Biology Education, College of Education, Chosun University, Gwangju 501-759, Republic of Korea.

Address correspondence to: Alexander van der Bliek ([avan@mednet.ucla.edu](mailto:avan@mednet.ucla.edu)).

Abbreviations used: CCCP, carbonyl cyanide *m*-chlorophenyl hydrazone; CFP, cyan fluorescent protein; ER, endoplasmic reticulum; GFP, green fluorescent protein; MAM, mitochondrion-associated membrane; PMA, phorbol-12-myristate-13-acetate; YFP, yellow fluorescent protein.

© 2014 Shen *et al.* This article is distributed by The American Society for Cell Biology under license from the author(s). Two months after publication it is available to the public under an Attribution-Noncommercial-Share Alike 3.0 Unported Creative Commons License (<http://creativecommons.org/licenses/by-nc-sa/3.0>). "ASCB®," "The American Society for Cell Biology®," and "Molecular Biology of the Cell®" are registered trademarks of The American Society of Cell Biology.

Supplemental Material can be found at:  
<http://www.molbiolcell.org/content/suppl/2013/11/04/mbc.E13-09-0525v1.DC1.html>

Mff is believed to be the principal recruitment factor for Drp1 on mitochondria in metazoans. Mff was shown to promote mitochondrial and peroxisome fission in mammalian cells (Gandre-Babbe and van der Blik, 2008) and subsequently to be the main Drp1 receptor (Otera *et al.*, 2010). MiD49 and MiD51 (MIEF1) proteins can act as alternative receptors because they also bind to Drp1 and affect fission when they are overexpressed or when their levels are altered in Mff-knockout cells (Loson *et al.*, 2013; Palmer *et al.*, 2013). Mff, MiD49, and MiD51 (MIEF1) proteins were shown to independently promote fission through Drp1 when they are expressed in a heterologous system (Koirala *et al.*, 2013). These experiments show that Mff, MiD49/Mief, and MiD51 proteins are distinct Drp1 recruitment factors. However, MiD49 and MiD51 (MIEF1) proteins are found only in vertebrates, whereas Mff is present in all metazoans, so it would appear that MiD49 and MiD51 (MIEF1) proteins provide a vertebrate-specific function during fission.

While studying the *Caenorhabditis elegans* fission proteins, we observed essential roles for Mff and Drp1 in stress-induced fission. These observations are consistent with earlier results showing that mitochondrial fission is needed to separate healthy from defective parts of mitochondria (Twig *et al.*, 2008). Moreover, genetic interactions between mutations in mitochondrial fission proteins and mutations in the Parkinson's proteins Pink1 and Parkin in *Drosophila* also suggest that mitochondrial fission is important for eliminating defective mitochondria (Deng *et al.*, 2008; Poole *et al.*, 2008; Yang *et al.*, 2008). Pink1 and Parkin are key regulators of mitophagy, which is a specialized form of autophagy. Pink1 is a serine threonine kinase that is normally imported into mitochondria and rapidly degraded. Pink1 import and degradation are blocked when damaged mitochondria lose their membrane potential. De novo-synthesized Pink1 is then shunted to the mitochondrial outer membrane, where it recruits the E3 ubiquitin ligase Parkin from the cytosol (Chan *et al.*, 2011; Youle and Narendra, 2011). Parkin-mediated ubiquitination leads to degradation of several key proteins, including mitofusins and Miro, which promote fusion between mitochondria and transport along microtubules (Youle and Narendra, 2011). By degrading these proteins, defective mitochondria are effectively isolated from the remaining population of mitochondria. It is not clear, however, to what extent and how directly mitochondrial fission proteins interact with mitophagy proteins.

Here we describe a new role for Fis1, acting in sequence with Mff. Fis1 mutants can still generate mitochondrial fragments upon treatment with stress-inducing chemicals, but the resulting autophagosomes form large LC3-positive aggregates that persist for many hours. Aggregate formation is inhibited by mutations in Drp1 and Mff and by mutations in Pink1, showing that Fis1 contributes to mitophagy. Chemicals that induce fission also promote interactions between Fis1, Drp1 and endoplasmic reticulum (ER) proteins, suggesting that Fis1 helps coordinate fission with changes in the ER-mitochondrial interface. We conclude that Fis1 acts after Drp1 and Mff initiate mitochondrial fission, guiding this process toward major cellular stress response pathways.

## RESULTS

### Effects of Fis1 and Mff on mitochondrial fission in *C. elegans*

To investigate the functions of Fis1 and Mff in *C. elegans*, we looked at strains with large deletions in each of the two *C. elegans* Fis1 and Mff genes. These were crossed, generating *fis-1(tm1867)*; *fis-2(gk414)* and *mff-1(tm2955)*; *mff-2(tm3041)* double mutants and a quadruple mutant with deletions in all four genes (hereafter called Fis1, Mff, and Fis1 Mff mutants). The effects on mitochondrial and peroxisome morphologies were compared with the strong fission

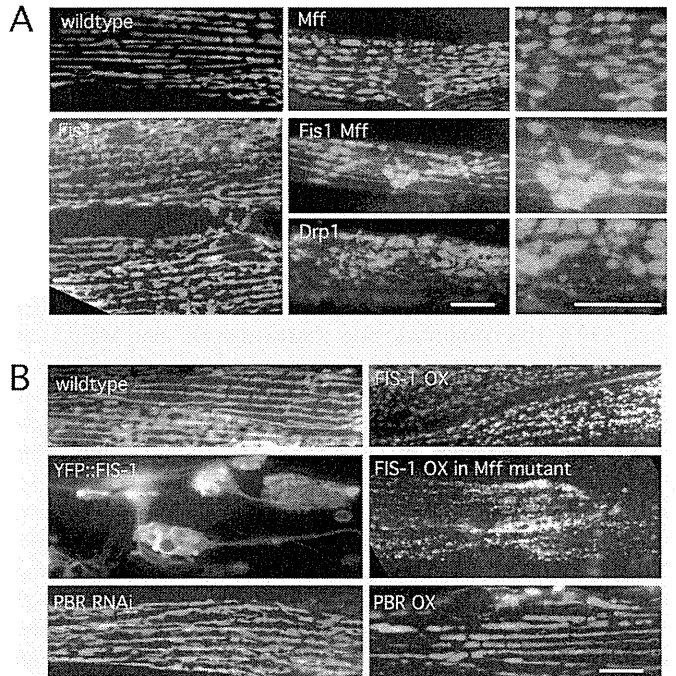


**FIGURE 1:** Effects of Mff and Fis1 on mitochondrial fission in *C. elegans*. (A) Mitochondria in *C. elegans* body wall muscles were labeled with mitochondrial outer membrane marker (YFP::Tom70, green) in strains as indicated. Right, enlargements of the Mff, Fis1 Mff, and Drp1 mutant images. (B) Effects of FIS-1 and YFP::FIS-1 overexpression with the muscle-specific myo-3 promoter. Mitochondria were labeled with YFP::TOM70. As a control for the effects of outer membrane proteins on mitochondrial morphology, we used feeding RNAi and an overexpression construct for another mitochondrial outer membrane protein (peripheral benzodiazepine receptor [PBR]). Bars, 10  $\mu$ m.

defects in the *drp-1(tm1108)* deletion strain. Our results show that *fis-1* and *fis-2* single and double mutants have wild-type mitochondrial morphologies, as also shown by others (Breckenridge *et al.*, 2008), that *mff-1* and *mff-2* single mutants have weak effects, and that the Mff double mutant has a mitochondrial fission defect similar to but not as strong as the *drp-1* defect (Labrousse *et al.*, 1999; Figure 1A and Supplemental Figure S1A). Analogous results were obtained with a peroxisome marker, showing punctate peroxisomes in wild-type and Fis1 mutants and tubular peroxisomes in *drp-1* mutant and Mff double mutants (Supplemental Figure S1B). We conclude that *C. elegans* Mff homologues affect mitochondrial and peroxisome fission, whereas Fis1 homologues have no obvious effects.

We tested whether Mff is essential for mitochondrial fission in *C. elegans*, as suggested for mammalian cells (Otera *et al.*, 2010), by inducing mitochondrial fission with the calcium ionophores ionomycin and A23187. These drugs convert mitochondria from their normal tubular shape to small, round, dispersed fragments in wild-type animals. As expected, calcium ionophore-induced fragmentation was not observed in *drp-1(tm1108)* mutants (Supplemental Figure S1C). However, fragmentation did occur in Fis1 and Mff double mutants and in the Fis1 Mff quadruple mutant, showing that Fis1 and Mff are not absolutely required for mitochondrial fission in *C. elegans* (Supplemental Figure S1C). To further test to what extent mutations in Fis1 or Mff inhibit mitochondrial fission, we conducted epistasis experiments with RNA interference (RNAi) for

mitochondrial fusion genes. The *drp-1* deletion completely reversed mitochondrial fragmentation caused by RNAi for the fusion proteins *fzo-1* and *eat-3* (Head *et al.*, 2011), but deletions in *Fis1* and *Mff* double mutants did not (Supplemental Figure S1, D and E). These results show that the effects of *C. elegans* *Mff* mutations are markedly less severe than the effects of a mutation in *drp-1*.

To test whether *Mff* mediates *Drp1* recruitment in *C. elegans*, as it does in mammals, we examined the localization of cyan fluorescent protein (CFP)::DRP-1 in muscle cells of mutant and wild-type animals. CFP::DRP-1 is observed in spots that mark impending fission events, as shown with time-lapse photography (Labrousse *et al.*, 1999). This pattern was also observed in *Fis1* and *Mff* double and *Fis1 Mff* quadruple mutants (Supplemental Figure S1F). Overexpression of CFP::DRP-1 changes mitochondrial morphologies in *Mff* double and *Fis1 Mff* quadruple mutants to a more normal tubular morphology, suggestive of *Drp1*-dependent fission without *Mff* (Supplemental Figure S1F). To verify that the different mutants have no effect on *Drp1* localization, we conducted subcellular fractionation. Western blots show similar amounts of DRP-1 in the mitochondrial fractions of wild-type, *Fis1* and *Mff* double mutants, and the *Fis1 Mff* quadruple mutant (Supplemental Figure S1G). *C. elegans* does not have *MiD49* or *MiD51* (*MIEF1*) homologues, which act as additional *Drp1* recruitment factors in vertebrates (Palmer *et al.*, 2011; Zhao *et al.*, 2011), but other factors may still exist. Alternatively, *Drp1* could bind directly to mitochondrial membranes, as suggested by *in vitro* binding to cardiolipin-containing liposomes (Montessuit *et al.*, 2010). We conclude that *Mff* affects fission, but *Mff* and *Fis1* are not essential for fission or for *Drp1* recruitment to mitochondria in *C. elegans*.

### Mutations in *Fis1* lead to LC3/LGG-1 aggregates

To further investigate the role of *Fis1*, we tested whether *Fis1* overexpression can induce mitochondrial fission in *C. elegans*. Our results show that *FIS-1* overexpressed with the *myo-3* promoter can cause fragmentation, similar to the effects of *Fis1* overexpression in mammalian cells (James *et al.*, 2003; Figure 1B). *FIS-1* overexpression also causes fragmentation in the *Mff* double mutant, showing that it is able to overcome an *Mff* deficiency. However, overexpression of a yellow fluorescent protein (YFP)-tagged version of *FIS-1* gives rise to grape-like clusters of mitochondria. These clusters are connected by thin tubules of mitochondrial outer membrane (Figure 1B). The few cells in which mitochondria are not clustered also have closed mitochondrial networks, suggesting that YFP::*FIS-1* interferes with the fission process. Overexpression of an unrelated mitochondrial outer membrane protein does not have this effect (Figure 1B). These dominant effects show that overexpressed *Fis1* can affect mitochondrial fission even though *C. elegans* *Fis1* proteins are not required for fission.

The grape-like clusters of mitochondria in cells with YFP::*FIS-1* are confined to small areas, unlike the dispersed mitochondrial distributions in wild-type animals and the *drp-1(tm1108)* mutant (Head *et al.*, 2011). These clusters resemble autophagosome intermediates (Yoshii *et al.*, 2011), which would be consistent with previous reports showing the induction of autophagy by overexpressed *Fis1* and the inhibition of mitophagy by *Fis1* small interfering RNA (siRNA) in mammalian cells (Gomes and Scorrano, 2008; Twig *et al.*, 2008). To test whether loss of *Fis1* function affects autophagy in *C. elegans*, we expressed the LC3 homologue LGG-1 fused to CFP in *Fis1* and *Mff* mutants. *Fis1* mutants showed a modest but consistent increase in the number and size of LGG-1::CFP clusters when compared with wild type or *Mff* mutants (Figure 2, A and B). This pattern was dramatically altered by treating worms for 1 h with the reactive

oxygen species (ROS)-producing chemical Paraquat, followed by a 5-h recovery. The small LGG-1 clusters in untreated cells were replaced by much larger clusters (Figure 2, A and B). Similar results were obtained when worms were treated with the mitochondrion-specific inhibitor antimycin A (Figure 2, A and B).

To determine whether the LGG-1 clusters in *Fis1* mutants contain remnants of mitochondria, we conducted triple labeling with the LGG-1 marker and mitochondrial outer membrane and matrix markers. Outer membrane and matrix markers were visible in inclusions in the LGG-1 aggregates, confirming that they contain portions of mitochondria (Supplemental Figure S2, A and B). Three-dimensional reconstructions of confocal images show that the aggregates consist of LGG-1 structures interspersed with mitochondria (Figure 2C). The aggregates disappear when *Fis1* is reintroduced with transgenic DNA, confirming that they are caused by mutations in *Fis1* (Supplemental Figure S2C). If the worms with aggregates were left to recover on plates without Paraquat, their aggregates persisted for many hours, but the mitochondrial marker (Tom70::YFP) disappeared over time (Supplemental Figure S2D), similar to the preferential degradation of mitochondrial outer membrane proteins in mammalian cells (Chan *et al.*, 2011; Sarraf *et al.*, 2013). CFP::DRP-1 was also initially present in and around the LGG-1 aggregates but then later disappeared (Supplemental Figure S2E). The aggregates disappear over the course of several days. It therefore seems likely that the aggregates are temporary structures formed by LGG-1-containing membranes that engulf portions of mitochondria. We conclude that mutations in *Fis1* affect autophagy in *C. elegans*, causing the formation of large aggregates containing LGG-1, DRP-1, and remnants of mitochondria.

### LC3/LGG-1 aggregates do not result from a compensatory response but instead are generated by aberrant mitochondrial fission

The large LGG-1 aggregates in *Fis1* mutants may result from stalled mitophagy intermediates or from an alternative autophagy pathway induced to compensate for the loss of *Fis1*. A compensatory mechanism would be consistent with the surprising lack of brood-size defects in *Fis1* mutants grown with increasing concentrations of Paraquat (Supplemental Figure S3A). We tested for compensatory mechanisms by growing *Fis1* mutants on *pha-4* and *daf-16* RNAi bacteria. These two genes encode the *FoxA* and *Foxo3* homologues, which are important transcriptional regulators of the major autophagic stress responses in *C. elegans* (Panowski *et al.*, 2007), but Paraquat still induces large LGG-1 aggregates in *Fis1* mutants grown with *pha-4* or *daf-16* RNAi (unpublished data), suggesting that these pathways are not required for aggregate formation. We also used quantitative PCR (qPCR) to determine the relative expression levels of autophagy genes controlled by *pha-4* and *daf-16*, but the expression levels of these genes in the *Fis1* double mutant was also similar to the expression levels in wild-type animals (Supplemental Figure S3B). These data show that genes encoding macroautophagy proteins are not induced in *C. elegans* *Fis1* mutants.

We used genetic interactions with other fission mutants to test whether the LGG-1 aggregates in *Fis1* mutants are by-products of faulty fission. The brood size of the *drp-1(tm1108)* deletion strain is reduced to zero when grown at 26°C instead of the normal temperature of 20°C (unpublished data). The brood size of the *Mff* double mutant is somewhat reduced at 26°C, and the brood size of the *Fis1* double mutant is the least affected (Supplemental Figure S3C), consistent with the different degrees to which mitochondrial fission is affected in these strains. Importantly, the reduction in brood size is no worse in the *Fis1 Mff* quadruple mutants

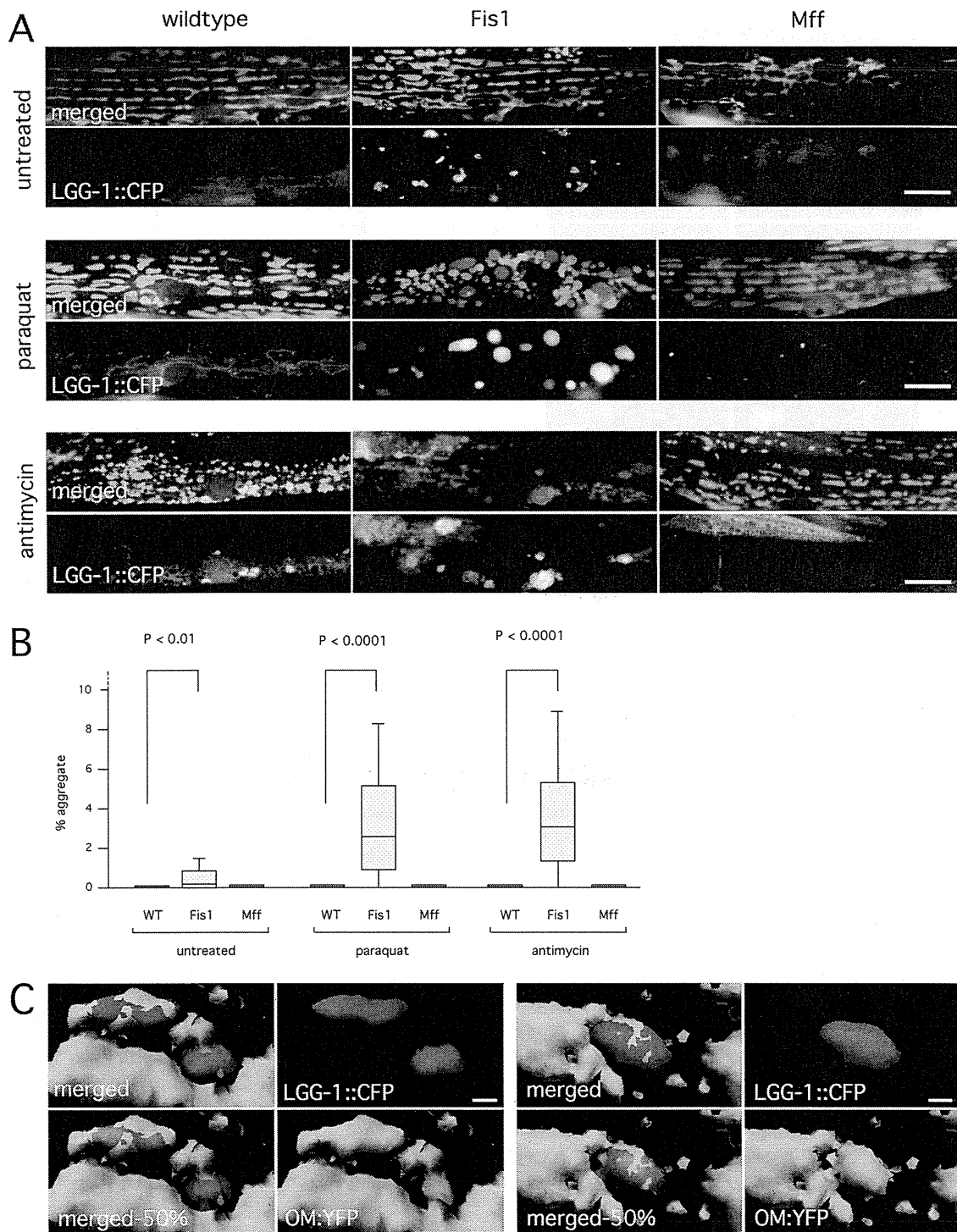


**FIGURE 2:** Fis1 genes trigger the formation of large autophagic aggregates. (A) CFP::LGG-1 (worm LC3, red) ectopically expressed in worm muscle cells along with YFP::TOM70 (green). Worms were untreated or incubated with Paraquat or antimycin A. Paraquat- and antimycin-treated worms were allowed to recover on plates without drugs (5 and 4 h, respectively). Bar, 10  $\mu$ m. (B) Aggregate sizes, shown as percentages of cell surface area. Box plots represent 40 or more cells per condition (*p* values determined with unpaired Student's *t* test). (C) Surface renderings of LGG-1 aggregates (red) and mitochondria (green) in a Fis1 mutant treated with Paraquat as in A, but without recovery time. Two examples. These renderings were made from confocal microscope images (stacks of 27 images with steps of 230 nm). Bottom left, opacity of the red channel set at 50% to visualize embedded mitochondria (labeled as merged-50%). Otherwise, opacity was set at 100%. Bar, 1  $\mu$ m.

than in the Mff mutants, even though Fis1 mutations by themselves also reduce brood size. These data show that there is no additive or synergistic effect of Fis1 and Mff mutations on brood size,

consistent with actions in the same pathway. This interpretation was confirmed by further analysis of LGG-1 aggregate formation at elevated temperatures. Wild-type and Mff mutants grown at 25 or